Article:
Moghaddam, H., Afzalinia, F. and Hajirasouliha, I. (2022) Optimal distribution of friction dampers to improve the seismic performance of steel moment resisting frames. Structures, 37. pp. 624-644. ISSN: 2352-0124

https://doi.org/10.1016/j.istruc.2022.01.007

Structures 37 (2022) 624–644

Contents lists available at ScienceDirect

Structures

journal homepage: www.elsevier.com/locate/structures

Optimal distribution of friction dampers to improve the seismic performance of steel moment resisting frames

Hassan Moghaddam [a], Farshad Afzalinia [a], Iman Hajirasouliha [b,*]

[a] Department of Civil Engineering, Sharif University of Technology, Tehran, Iran
[b] Department of Civil & Structural Engineering, The University of Sheffield, Sheffield, UK

ARTICLE INFO

Keywords:
Friction damper
Optimisation
Performance-based design
Steel moment resisting frames
Time history analysis

ABSTRACT

This study aims to develop a low computational cost framework to optimize the seismic performance of the steel moment-resisting frames (SMRFs) equipped with friction dampers at different performance levels. To achieve the optimal design of dampers in a structure, a novel approach called adaptive optimisation technique (AOT) is adopted. The basis of this method is to achieve a uniform distribution of damage (UDD) in the structure to exploit the maximum energy dissipation capacity of the dampers. The optimisation objective is to obtain the best position of friction dampers and minimize their slip-threshold force to satisfy a predefined inter-story drift (i.e. selected performance target). The efficiency of the proposed method is demonstrated through optimum design of 4, 8, and 16-story SMRFs subjected to a set of strong natural earthquake records. The unique features of AOT are examined including the high convergence rate, the independence of the optimal solution from an arbitrary starting point, and also the ability to perform multi-level performance optimisation. Finally, the dependency of the seismic optimisation methods to the selected design acceleration record, as a challenge in the practical seismic design process, is addressed by proposing a modification in the proposed adaptive formula. In addition, the results of the proposed method are compared with iterative, non-iterative, and some metaheuristic optimisation methods such as genetic algorithm (GA), particle swarm optimisation algorithm (PSO), and simulated annealing algorithm (SA). It is shown that the AOT can lead to optimum design solutions with significantly less computational costs (up to 98%) compared to the conventional techniques.

1. Introduction

Passive energy dissipation devices are increasingly employed to improve the seismic response of both existing and new design structures by absorbing a significant portion of the earthquake input energy. The beneficial effects of supplemental passive dampers have been investigated in the past [1-5]. Passive dampers contain different types such as metallic, frictional, viscoelastic, viscous, tuned mass and tuned liquid. Among these, friction dampers can provide cost-efficient and easy-tuned design solutions in most cases. The behavior of friction dampers is generally based on the friction between two pre-stressed surfaces. Once the imposed force reaches the pre-stressing level, the surfaces are ready to slide and dissipate energy. The idea of using friction dampers in building structures was first introduced by Pall [6]. He considered a frictional connection with a limited-slip length between two concrete panels to reduce the seismic response. It was shown that, in general, the cyclic behavior has a rectangular shape that corresponds to the Coulomb's law. Pall [6] considered four stages for the frictional action: elastic range, slip, hardening due to locking of the bolt, and hitting the end of the groove.

Roik et al. [7] studied the frictional behavior between steel and concrete and suggested a 3-element connection, in which each element represented one of the foregoing stages. Although their model could take into account the non-linearity in the vicinity of the transition zones from one phase to another, it could not predict the sudden increase in the developed force due to the interconnected bolt collision. In another relevant study, Lukkunaprasit et al. [8] showed that the collision of bolts with the end of the grooves imposes another nonlinear phase, while the amount of the collision force depends on the shear capacity of the bolts. In addition, some of the pre-stressed forces dissipate due to the collision, which leads to a reduction in the area of the hysteresis loops and hence the energy dissipation capacity of the dampers.

Different types of friction connections have been used to enhance the seismic performance of the structures, such as friction diagonal bracings

* Corresponding author.
E-mail address: i.hajirasouliha@sheffield.ac.uk (I. Hajirasouliha).

https://doi.org/10.1016/j.istruc.2022.01.007
Received 1 November 2021; Received in revised form 29 December 2021; Accepted 4 January 2022
Available online 20 January 2022

(e.g. [9-12]), friction walls (e.g. [13-17]) and friction beam-to-column joints (e.g. [18-20]). The results of these studies, in general, demonstrated the excellent performance of friction-dampers in improving the seismic performance of structures by reducing the displacement demands and the energy absorbed in the structural elements. The friction diagonal bracings have the advantage to provide both high lateral stiffness (before slippage) and energy dissipation capacity. However, if they are not designed properly, they may lead to concentrated damage at the connections of the brace elements. The buckling of the brace elements under compression loads can be also an issue [9-12]. These shortcomings can be sufficiently addressed by using friction wall systems such as those proposed by Nabid et al. [13-17]. However, the friction wall dampers are more suitable for RC structures. As another viable solution, friction beam-to-column joints have been proposed to improve the seismic performance of steel moment-resisting frames (SMRFs) [18-20]. Nastri et al. [18] showed that these connections can be designed to be fully rigid while they also provide a highly ductile behaviour. In other relevant studies, Di Lauro et al. [19] evaluated the over-strength coefficient and partial safety factors to design friction beam-to-column connections, while Tartaglia et al. [20] demonstrated that their dissipative response is not generally affected by the size of connected members. Longo el al. [21] and Montuori et al. [22] developed the theory of plastic mechanism control for moment resisting frames combined with concentrically braced frames (MRF-CBF). The aim was to design the structures to fail in global modes. In a follow-up study, Piluso et al. [23] investigated the seismic performance of these dual systems when they are equipped with low damage friction connections. The results of their study indicated that the proposed system exhibited excellent seismic performance by preventing yielding of primary structural elements under the design earthquake.

The present research focuses on the design of friction dampers that are installed in diagonal bracing elements of steel moment resisting frames (SMRFs), as one of the most widely used systems in common practice. The two key factors in the design of friction dampers are the slip-threshold forces and the effective location arrangement. To optimize the performance of friction dampers, their best positions within the structure and the optimum slip-threshold forces corresponding to these positions should be determined simultaneously. Baktash and Marsh [10] attempted to optimize the threshold force by minimizing the difference between the input and output energy. The difference between input and output energy is presented as a mathematical function, which is used to determine the number of dampers required in each story level. The derivative of this function is set to zero, and the optimal slip force for each floor is calculated as follows:

$$V_{br,j} = \frac{V_{f\&br,j}}{2}\left[\sin^2\theta_j + \left(\frac{K_{br,j}}{K_{f\&br,j}}\right)\cos^2\theta_j\right] \tag{1}$$

where $V_{f\&br,j}$ and $K_{f\&br,j}$ are the story shear force and stiffness of the j^{th} level of the frame, respectively, while $V_{br,j}$ and $K_{br,j}$ are the bracing share of the shear force and stiffness of the brace at the same level, respectively. θ is the angle of the brace element relative to the X-axis.

Moreschi [11] attempted to optimize the slip threshold force of a friction damper based on a relative performance index (RPI) defined as follows:

$$RPI = \frac{1}{2}\left(\frac{SEA}{SEA_{(0)}} + \frac{U_{max}}{U_{\max(0)}}\right) \tag{2}$$

where SEA and U_{max} are the cumulative strain energy and the maximum strain energy of the structure with supplemental friction damper, respectively, and $SEA_{(0)}$ and $U_{max(0)}$ are the same values for the structure without damper. Moreschi [11] presented the average optimisation results for 4 accelerations using the genetic algorithm, while minimizing the RPI index was considered as the objective function. The complexity of the objective function and the necessity of using dampers in all stories levels as a constraint are some of the disadvantage of this method for practical applications. In another relevant study, Sung-Kyung Lee et al. [12] used the following two coefficients to distribute dampers in different stories, assuming the ratio of brace stiffness to the story stiffness to be equal to 2:

ρ_1 = slip load / maximum shear force of the undamped building

ρ_2 = slip load / maximum shear force of each story of the undamped building

It is clear that ρ_1 leads to the distribution of the same dampers in the stories, while ρ_2 leads to the distribution of dampers proportional to the inter-story shear of each story. To obtain the best distribution of dampers, starting from zero and increasing these coefficients with 0.05 increment at each stage, the seismic performance of the frame was evaluated using the following two indices:

$$R_d = \frac{max_{i=1,..,n}\left\{|\delta_s(t)|_{max}\right\}}{max_{i=1,..,n}\left\{|\delta(t)|_{max}\right\}} \tag{3}$$

$$R_a = \frac{max_{i=1,..,n}\left\{\left|\ddot{Y}_s(t)\right|_{max}\right\}}{max_{i=1,..,n}\left\{\left|\ddot{Y}(t)\right|_{max}\right\}} \tag{4}$$

where R_d and R_a are the ratios of the damped response to the undamped response; $\delta_s(t)$ and $\delta(t)$ represent the damped and undamped inter-story drifts, respectively; and $\ddot{Y}_s(t)$ and $\ddot{Y}_s(t)$ are the damped and undamped

Table 1
Sections of beams and columns.

story	4-story frame			8-story frame			16-story frame		
	beam	interior column	exterior column	beam	interior column	exterior column	beam	interior column	exterior column
1	W33 × 130	W14 × 311	W14 × 233	W30 × 124	W14 × 342	W14 × 283	W36 × 160	W14 × 550	W14 × 426
2	W27 × 114	W14 × 311	W14 × 193	W30 × 116	W14 × 257	W14 × 159	W36 × 160	W14 × 500	W14 × 398
3	W27 × 94	W14 × 176	W14 × 99	W30 × 116	W14 × 257	W14 × 145	W36 × 160	W14 × 455	W14 × 398
4	W24 × 68	W14 × 74	W14 × 74	W30 × 108	W14 × 233	W14 × 132	W36 × 160	W14 × 455	W14 × 342
5				W27 × 102	W14 × 211	W14 × 109	W36 × 150	W14 × 455	W14 × 342
6				W21 × 93	W14 × 176	W14 × 109	W36 × 150	W14 × 426	W14 × 283
7				W21 × 83	W14 × 132	W14 × 99	W36 × 150	W14 × 398	W14 × 283
8				W18 × 60	W14 × 99	W14 × 99	W36 × 150	W14 × 398	W14 × 283
9							W33 × 130	W14 × 370	W14 × 283
10							W33 × 130	W14 × 311	W14 × 257
11							W33 × 130	W14 × 311	W14 × 257
12							W33 × 130	W14 × 311	W14 × 176
13							W30 × 116	W14 × 283	W14 × 145
14							W30 × 116	W14 × 283	W14 × 132
15							W30 × 116	W14 × 283	W14 × 132
16							W30 × 116	W14 × 132	W14 × 120

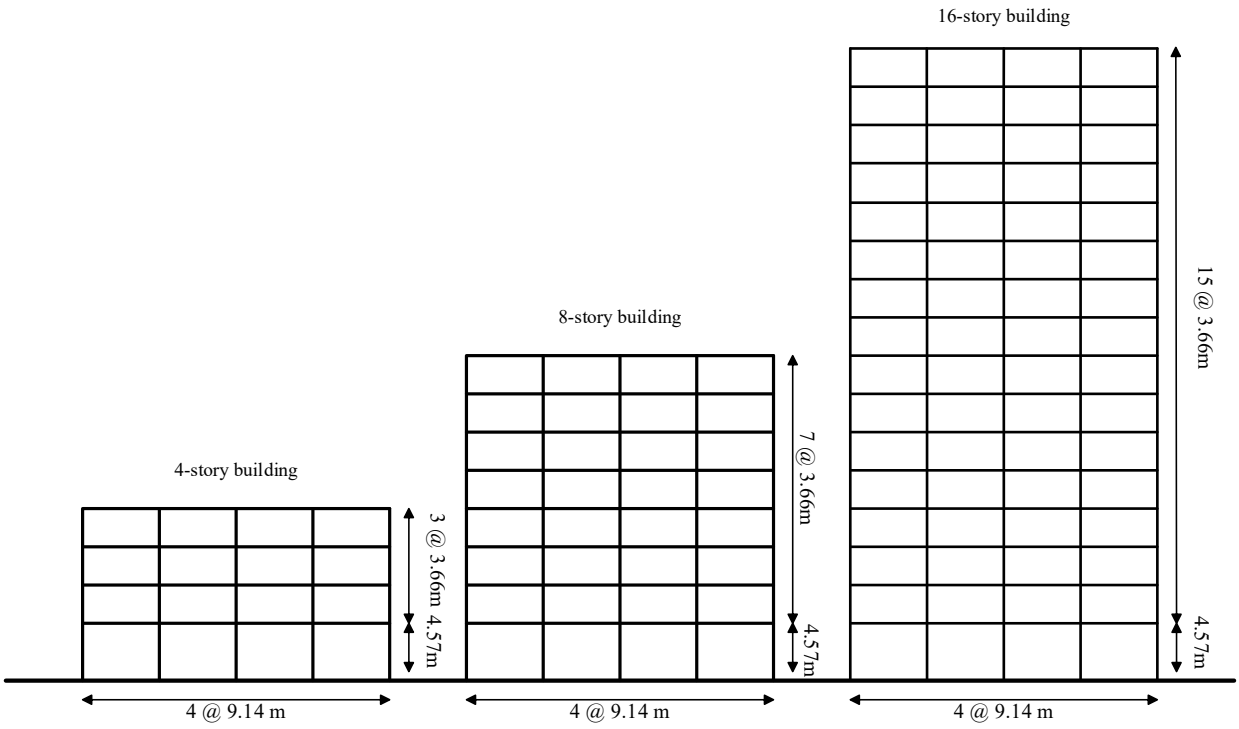

Fig. 1. The reference 4, 8 and 16-story frame models.

Table 2
Far field seismic records selected from FEMA P695 list.

No.	PEER ID	EQ Name	Station name	M	PGA(g)	NEHRP Class	Vs_30 (m/sec)	Distance (km)
1	953	Northridge	Beverly Hills - Mulhol	6.7	0.488	D	356	13.3
2	960	Northridge	Canyon Country-WLC	6.7	0.472	D	309	26.5
3	1602	Duzce,Turkey	Bolu	7.1	0.806	D	326	41.3
4	1787	Hector Mine	Hector	7.1	0.328	C	685	26.5
5	169	Imperial Valley	Delta	6.5	0.35	D	275	33.7
6	174	Imperial Valley	El Centro Array #11	6.5	0.379	D	196	29.4
7	1111	Kobe,Japan	Nishi-Akashi	6.9	0.483	C	609	8.7
8	1116	Kobe,Japan	Shin-Osaka	6.9	0.233	D	256	46
9	1158	Kocaeli,Turkey	Duzce	7.5	0.364	D	276	98.2
10	1148	Kocaeli,Turkey	Arcelik	7.5	0.21	C	523	53.7
11	900	Landers	Yermo Fire Station	7.3	0.245	D	354	86
12	848	Landers	Coolwater	7.3	0.417	D	271	82.1
13	752	Loma Prieta	Capitola	6.9	0.511	D	289	9.8
14	767	Loma Prieta	Gilroy Array #3	6.9	0.559	D	350	31.4
15	1633	Manjil,Iran	Abbar	7.4	0.515	C	724	40.4
16	721	Superstition Hills	El Centro Imp. Co.	6.5	0.357	D	192	35.8
17	725	Superstition Hills	Poe Road (temp)	6.5	0.475	D	208	11.2
18	829	Cape Mendocino	Rio Dell Overpass	7	0.55	D	312	22.7
19	1244	Chi-Chi,Taiwan	CHY101	7.6	0.398	D	259	32
20	1485	Chi-Chi,Taiwan	TCU045	7.6	0.507	C	705	77.5
21	68	San Fernando	LA - Hollywood Stor	6.6	0.225	D	316	39.5
22	125	Friuli,Italy	Tolmezzo	6.5	0.357	C	425	20.2

absolute accelerations, respectively. Finally, the optimal distribution of dampers was obtained by minimizing the values of R_d and R_a. Sung-Kyung Lee et al. [12] also concluded that R_d leads to more appropriate and stable solutions for friction dampers.

It should be noted that all the above mentioned methods to determine the optimal slip force and location of friction dampers under earthquake excitations are computationally expenses, especially in the case of large scale structures. To address this challenge, the principle of uniform distribution of damage (UDD) has been used in recent studies by Nabid et al. [13-17] for the efficient distribution of frictional wall dampers in RC frames which resulted in some practical empirical design equations. However, the results of their study are not applicable for other types of structural systems and damping arrangements. This highlights the need to develop more practical methods for optimum performance-based design and placement of friction dampers that are installed in bracing elements of steel moment resisting frames as one of the most widely used structural systems in common practice. To bridge this research gap, this study aims to propose a novel low-computational cost framework for multi-level performance optimisation of such systems for the first time. The optimisation objective is to obtain the best position of friction dampers and minimize their slip-threshold force to satisfy a predefined performance target (here expressed in terms of limits on maximum inter-story drifts). This will lead to a design solution with minimum additional forces imposed by dampers to the adjacent structural elements. However, the strength capacity of the frame elements is also checked in the final design solution to ensure their

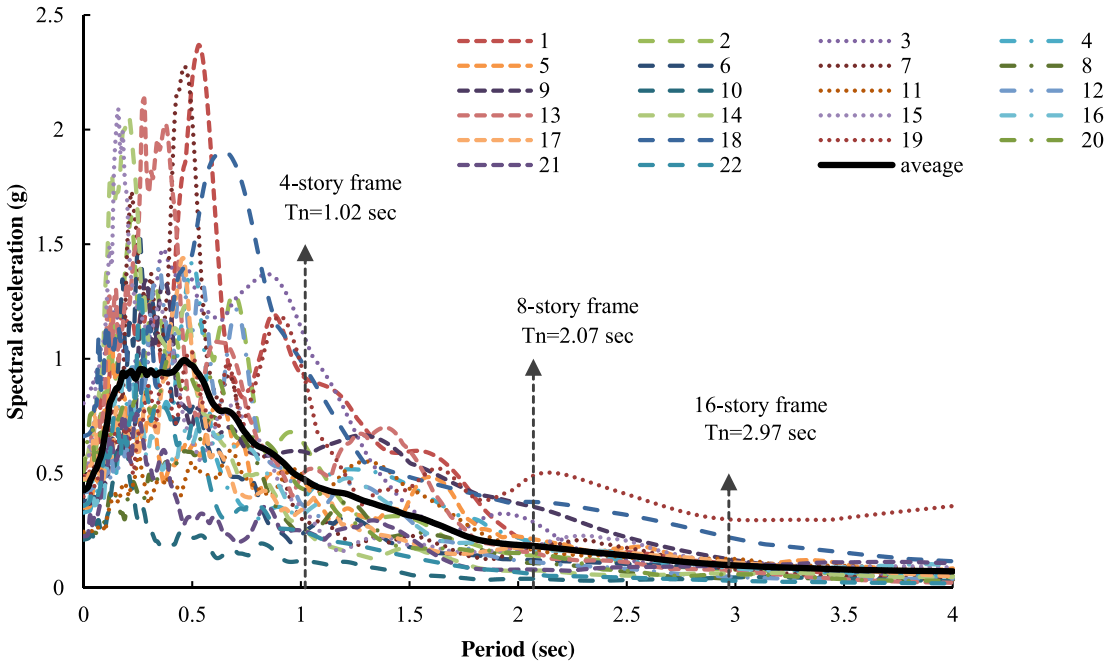

Fig. 2. Acceleration response spectra of the selected records.

adequacy. The efficiency of the proposed method is then demonstrated for 4, 8, and 16-story SMRFs subjected to a set of strong natural earthquake records. While this study only considers friction dampers that are installed in diagonal bracing elements, the proposed methodology is general and can be easily adopted for other types of friction dampers.

2. Methods

2.1. Adaptive optimisation technique (AOT)

The concept of the AOT used in the present study has been initially developed for the optimum seismic design of the structures by the first author in 1996 [24]. It was shown that there is no need to use a specific pattern for seismic forces in a seismic design. Instead, the structure was subjected directly to the seismic excitation, and the structural members were modified according to their actual responses. This approach is inspired by the natural adaptation of the body where those parts that are under more pressure become stronger and vice versa, and can be outlined as follows:

1. There is no need to consider either any seismic load, or load pattern. However, a primary seismic resistant system is required.
2. The primary design should sustain gravity loads regardless of seismic forces.
3. The structure is subjected to the given seismic excitation representing the design spectrum.
4. The force-controlled members are modified so to sustain the calculated internal force.
5. The deformation-controlled members are modified according to the following adaptation Equation:

$$(P_{sc})_1 = (P_{sc})_0 . f(\frac{\delta}{\delta_t}) \tag{5}$$

where P_{sc} is the selected performance parameter to control the seismic response of the member. Subscripts 1 and 0 represent the current and previous steps of analysis, respectively. The adaptive function f directly depends on the ratio δ/δ_t, where δ and δ_t are the calculated and the target deformation demands, respectively.

In general, the adaptive function f can be presented as any mathematical function that can close the gap between the deformation demand (δ) and the target demand (δ_t) by modifying the key design parameters of the members. However, to improve the convergence of the optimisation problem and avoid instability in the analysis, any changes in the structural properties should be gradual [25]. A good example of the such functions, which has been successfully used for different types of structural members, is as follows [26,27]:

$$f(\frac{\delta}{\delta_t}) = (\frac{\delta}{\delta_t})^{\beta} \tag{6}$$

The convergence coefficient, β, controls the stability and convergence of the optimisation process and has a significant influence on the convergence rate. It is noteworthy that increasing β has a mixed effect as it increases both the convergence rate and the tendency for fluctuation. While an appropriate value of β depends on the type of structure, different ranges have been proposed in previous studies including: 0.1 to 0.2 proposed by Hajirasouliha et al. [28] for RC frames, 0.4 to 0.8 suggested by Mohammadi et al. [29] for steel frames with metallic-yielding dampers, 0.2 to 0.5 suggested by Nabid et al. [16] for RC frames with friction dampers, 0.5 recommended by Lavan [30] for nonlinear structures with viscous dampers, and less than 0.02 suggested by Moghaddam et al. [31] for moment resisting steel frames.

2.2. Application of adaptive optimisation technique for friction dampers

The concept of the adaptive optimisation technique has been used for optimum design of a variety of structures such as shear buildings, braced and moment resisting steel frames, reinforced concrete frames, and truss structures [28,32-40]. In order to apply adaptive optimisation technique for optimizing the friction dampers, maximum inter-story drift and slip threshold force of friction damper is considered as deformation parameter and behavioral parameter, respectively. The gradual changes to the dampers at each step will be achieved using the following equation:

$$\left[(P_{sc})_i\right]_{n+1} = \left[(P_{sc})_i\right]_n . \left(\frac{Drift_{max}}{Drift_{target}}\right)^{\beta} \tag{7}$$

where P_{sc} is the behavioral parameter, $Drift_{max}$ is the maximum inter-

story drift in each step, and $Drift_{target}$ is the target drift assumed as equal to 1% based on immediate occupancy level (IO) in ASCE/SEI 41–13 [41]. Analyses conducted in this study show that a range of 0.4 to 0.8 values for the convergence coefficient, β, will guarantee the convergence in the case of optimisation of friction dampers.

In this study, three 4, 8, and 16-story steel moment resisting frames (SMRFs) were considered to demonstrate the efficiency of the proposed optimisation method. It should be mentioned that these reference frames have been also used by Jin and El-Tawil [42], Ghassemieh and Kiani [43], Kildashti et al. [44], and Naughton et al. [45]. All the three building models have identical square floor plans, 4 spans of 9.14 m in each direction, with an area of 1336 m^2 (36.25 × 36.25 m). The height of the first floor is 4.57 m, while the height of the other floors is equal to 3.66 m. The dead and live loads are 3.64 KN/m^2 and 0.96 KN/m^2, respectively, for the roof, and 5.55 KN/m^2 and 2.39 KN/m^2, respectively, for the floors. All beam and column members are made of A572 grade50 steel with the yield strength of approximately equal to 345 MPa. In these structures, the perimeter frames solely resist the lateral loads and therefore are modelled to assess the seismic performance of the systems. Since there are two perimeter frames in each direction, each frame is associated with half of the total mass of the structure. All the supports and beam-to-column connections are assumed to be fixed. Both P-δ and P–Δ effects are taken into account in the analyses and the diaphragms are considered to be rigid. These frames are designed in compliance with FEMA302 [46], FEMA350 [47] and AISC 341–16 [48], by considering the principle of the strong column-weak beam. The designed sections for beams and columns are presented in Table 1.

In order to model these frames, the finite element software, OpenSees [49] is used to conduct nonlinear time history analyses. The nonlinear behaviour of the beam and column elements are simulated by using the distributed plasticity fibre-based "nonlinearBeamColumn element" model in OpenSees [49]. The adopted distributed plasticity model allows yielding to occur at any location along the elements. To model the nonlinear response of each fiber section, the bilinear "Steel02" uniaxial material model is used, while the strain hardening ratio is assumed to be 3%. Seven integration points are considered along the element based on Gauss-Lobatto quadrature rule. It is assumed that all of the lateral forces applied to the building are resisted by the perimeter SMRFs and the internal frames bear only the gravity loads. Since the perimeter frames are identical in both directions, a two-dimensional frame is modeled and analyzed under lateral loads. The schematic configuration of model frames is shown in Fig. 1. For nonlinear dynamic analyses, 5% damping ratio is considered using the Rayleigh damping model.

2.3. Ground motions

In this study, 22 earthquake records listed in Table 2 are selected from FEMA P695 [50]. The specifications of these records are taken from PEER database [51] and their response spectra are illustrated in Fig. 2. All these ground motions were recorded on soil type C and D in accordance to NEHRP [52] and represent earthquakes with high local magnitudes (i.e. rapture distance over Ms > 6.5). The average spectrum of these records is considered to represent the Design-Basis Earthquake (DBE), and therefore, these records are used without scaling (see Fig. 2).

3. Results and discussion

3.1. Optimisation for a design compatible earthquake excitation

To investigate the efficiency of the proposed adaptive optimisation technique, an arbitrary distribution of friction dampers is considered as the starting point. It is assumed that there is a weak damper at each story with a slip threshold force of 20KN. Considering that the frames have 4 spans, in order to maintain symmetry, the slip threshold force of each story is distributed to two friction dampers in two mid-spans in symmetrical form as shown in Fig. 3.

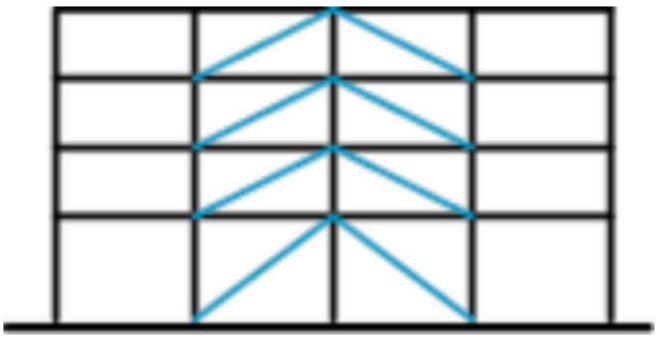

Fig. 3. Distribution of dampers in frames.

The Optimisation process is carried out for the frames until the optimal distribution of dampers is reached. In this study, the criterion for the convergence is considered to achieve a coefficient of variation (COV) of maximum inter-story drift less than 0.05. The COV of maximum inter-story drifts is calculated according to Equation (8). The reduction of this coefficient results in more uniformity in the maximum inter-story drift, which is expected to lead to more efficient use of structural capacity considering the concept of uniform damage distribution (UDD).

$$COV = \frac{1}{Drift_{target}} \sqrt{\frac{1}{n-1} \sum_{i=1}^{n} \left(\left(Drift_{max} \right)_i - \left(Drift_{target} \right)_i \right)^2} \tag{8}$$

The proposed Optimisation process (see Section 2.2) is performed for a selected acceleration record (No. 2) and the results are presented in Fig. 4. The convergence coefficient, β, was considered to be 0.8. As it is evident from these figures, the distributions of slip threshold force of friction dampers are not the same and in some stories, dampers have even been eliminated which is one of the important advantages of the adaptive optimisation technique. The summation of all damper threshold forces (dampers weight) is considered as a cost function in this study. The variation of dampers weight throughout the optimisation process, shown in Fig. 4(b), indicates that the convergence was achieved in all cases in less than 20 steps without any fluctuations. The maximum inter-story drifts before and after optimisation are also compared in Fig. 4(c). It is shown that in the optimum structures, the maximum drift is always equal to or less than the target value (i.e. IO limit, 1%).

3.2. Effects of initial distribution of dampers

To investigate the effect of initial distribution of slip threshold force of friction dampers (used as starting point of the optimisation process) on the final design solutions, two different initial distributions, including relatively weak dampers and relatively strong dampers in all stories are considered. The optimisation process is then carried out for each of these two cases separately. Fig. 5 shows the variation of the dampers weight and COV of maximum inter-story drifts for each of the initial distributions during the optimisation process of 4, 8 and 16-story frames. It can be seen that in all the cases, the dampers weight converges to an identical value, indicating that the final solution is not affected by starting point. In order to generalize this assertion, several other initial distributions have been also used as listed in Tables 3–5. Fig. 6 shows the convergence trend of dampers weight for different starting points. The results confirm that for all the designed frames, the dampers weight converged to the same final solution, irrespective of the selected initial distribution of slip threshold forces. However, it is shown that the convergence rate can be affected by the selected starting point.

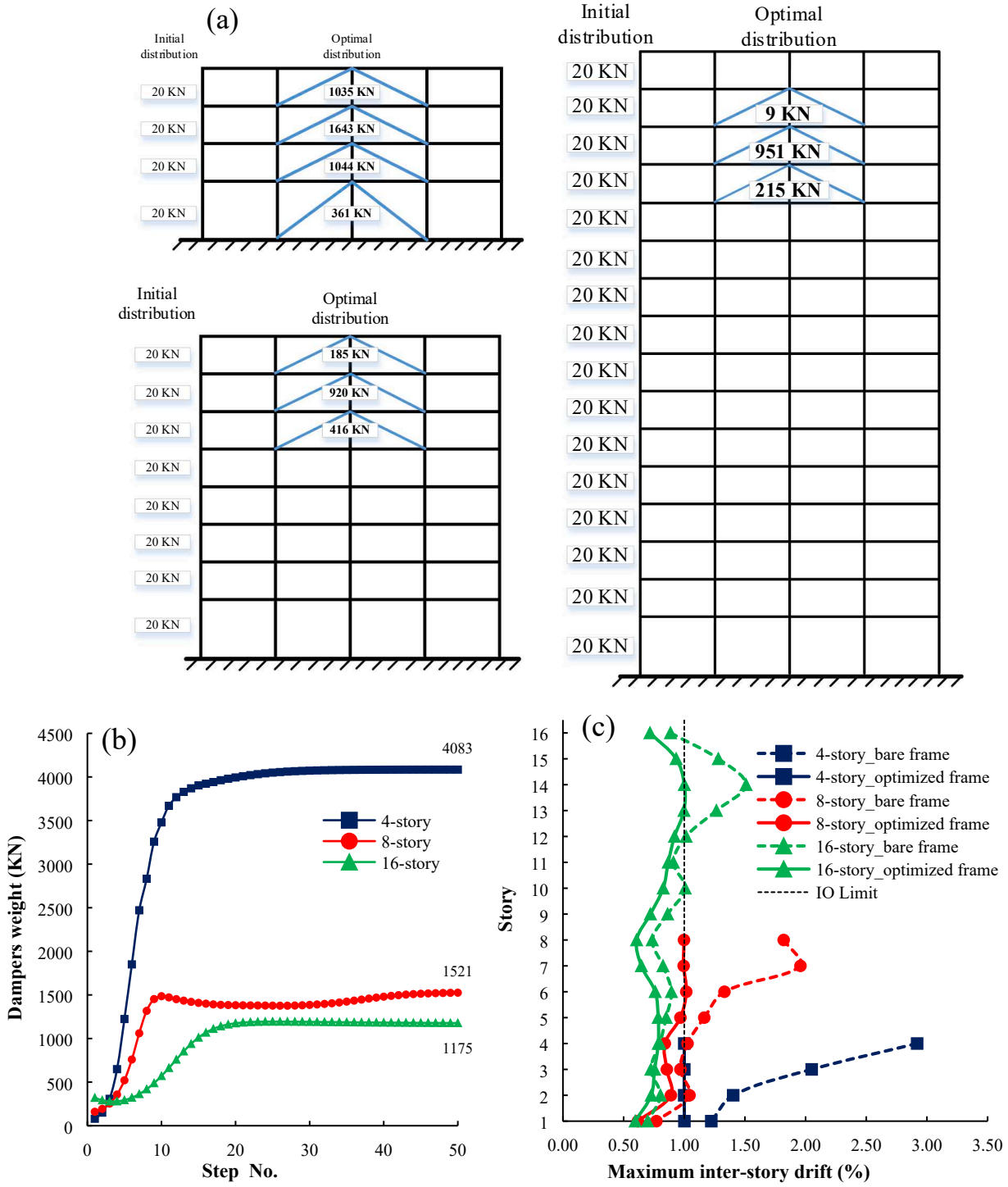

Fig. 4. (a) Initial and optimal distribution of dampers using $\beta = 0.8$; (b) convergence trend of dampers weight; (c) maximum inter-story drifts before and after optimisation.

3.3. *Multi-level performance-based optimisation*

In this section, optimisation of slip threshold force and the effective location of dampers is carried out by considering the seismic performance of the frames under two earthquake intensity levels simultaneously. The optimisation criteria in this case can be expressed as:

- Maximum inter-story drift under earthquake level A, reaches the target value of this level.
- Maximum inter-story drift in the earthquake level B, reaches the target value of this level.

It should be noted that these two criteria are not in the same direction, and achieving one does not necessarily satisfy the other one. To deal with this two-level optimisation problem, the adaptation factor used in equation (5) is defined as follows:

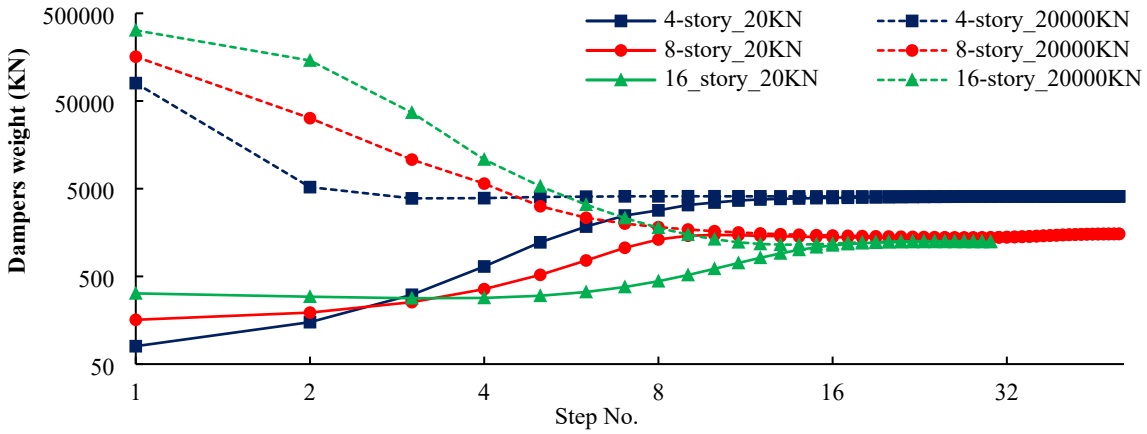

Fig. 5. Convergence process of dampers weight using two different initial distribution of dampers for 4, 8 and 16-story frames.

Table 3
Assumed values for different initial distribution of dampers in 4-story.

Story	Uniform1	Uniform2	Triangular1	Triangular2	Triangular3	Random1	Random2	Random3
1	20	20,000	3000	0	0	21,000	8700	790
2	20	20,000	2000	1000	2000	5000	1700	30
3	20	20,000	1000	2000	2000	93,000	6100	170
4	20	20,000	0	3000	0	45,000	3800	650
Dampers weight(KN)	80	80,000	6000	6000	4000	164,000	20,300	1640

Table 4
Assumed values for different initial distribution of dampers in 8-story.

Story	Uniform1	Uniform2	Triangular1	Triangular2	Triangular3	Random1	Random2	Random3
1	20	20,000	7000	0	0	35,000	8600	400
2	20	20,000	6000	1000	2000	11,000	7300	780
3	20	20,000	5000	2000	4000	93,000	300	250
4	20	20,000	4000	3000	6000	57,000	1700	590
5	20	20,000	3000	4000	6000	8000	4800	130
6	20	20,000	2000	5000	4000	88,000	1900	970
7	20	20,000	1000	6000	2000	67,000	7400	420
8	20	20,000	0	7000	0	49,000	5800	630
Dampers weight(KN)	160	160,000	28,000	28,000	24,000	408,000	37,800	4170

Table 5
Assumed values for different initial distribution of dampers in 16-story.

Story	Uniform1	Uniform2	Triangular1	Triangular2	Triangular3	Random1	Random2	Random3
1	20	20,000	15,000	0	0	18,000	8700	390
2	20	20,000	14,000	1000	2000	42,000	2100	860
3	20	20,000	13,000	2000	4000	11,000	900	140
4	20	20,000	12,000	3000	6000	57,000	3900	280
5	20	20,000	11,000	4000	8000	91,000	6700	780
6	20	20,000	10,000	5000	10,000	22,000	4300	490
7	20	20,000	9000	6000	12,000	69,000	3700	110
8	20	20,000	8000	7000	14,000	63,000	6100	670
9	20	20,000	7000	8000	14,000	85,000	400	180
10	20	20,000	6000	9000	12,000	8000	8000	290
11	20	20,000	5000	10,000	10,000	74,000	5900	470
12	20	20,000	4000	11,000	8000	33,000	3200	60
13	20	20,000	3000	12,000	6000	12,000	4600	190
14	20	20,000	2000	13,000	4000	44,000	1700	920
15	20	20,000	1000	14,000	2000	81,000	8800	310
16	20	20,000	0	15,000	0	58,000	9700	170
Dampers weight(KN)	320	320,000	120,000	120,000	112,000	768,000	78,700	6310

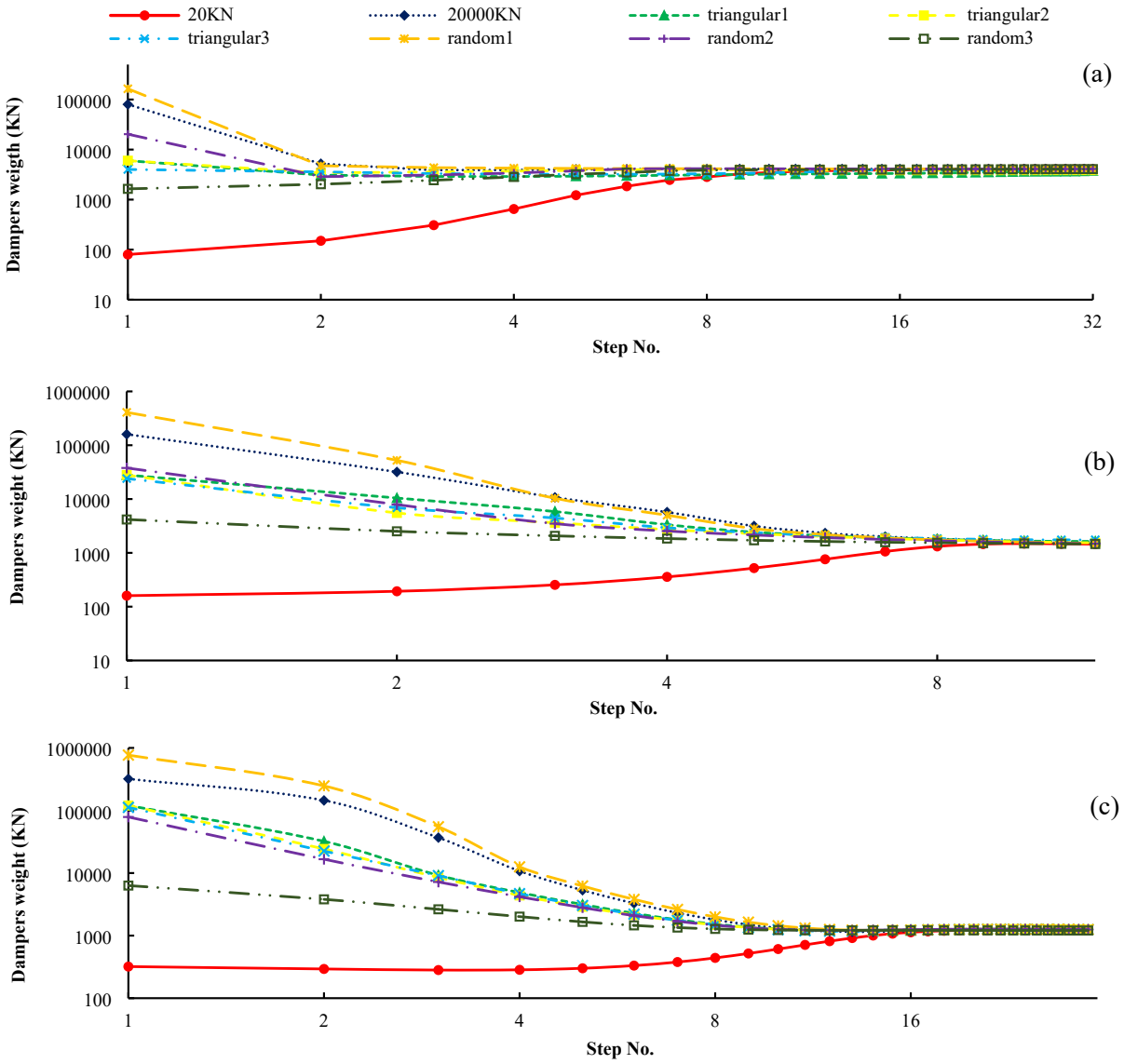

Fig. 6. Convergence trend of dampers weight in different starting points: (a) 4-story frame; (b) 8-story frame; (c) 16-story frame.

$$f\left(\frac{\delta}{\delta_t}\right)_i = \left(max\left\{\left(\frac{(Drift_{max})_A}{(Drift_{target})_A}\right)_i, \left(\frac{(Drift_{max})_B}{(Drift_{target})_B}\right)_i\right\}\right)^{\beta} \quad (9)$$

where $(Drift_{max})_A$ and $(Drift_{max})_B$ are maximum inter-story drift under earthquake level A and B, respectively, while $(Drift_{target})_A$ and $(Drift_{target})_B$ are target inter-story drift under earthquake intensity levels A and B, respectively.

In order to apply the adaptive optimisation technique for two-level optimisation in this study, it is assumed that levels A and B represent PGA = 0.3 g and PGA = 0.8 g, respectively. The target drifts for earthquake intensity levels A and B are assumed to be 1% and 2.5%, respectively (according to Immediate Occupancy and Life Safety limits in ASCE/SEI 41–13). To achieve earthquake intensity levels A and level B, one of the above mentioned acceleration records (record No. 9) is scaled to PGA = 0.3 g and PGA = 0.8 g, respectively. Then, an arbitrary distribution pattern for dampers is considered and the structure is analyzed under earthquake intensity levels A and B separately. The maximum inter-story drifts are then obtained and the adaption factor of each story is calculated according to Equation (9). Subsequently, the slip threshold force of the dampers in each story are modified according to Equation (7). This process continues until dampers weight converges to a unique value. Figs. 7(a), 8(a), and 9(a) show the optimal distribution of the dampers in each frame, while Figs. 7(b), 8(b), and 9(b) illustrate the convergence process of dampers weight in each case. As shown in Figs. 7(c) to 9(c) and 7(d) to 9(d), the maximum inter-story drifts of the frames under earthquake intensity level A and B is equal to or less than 1% and 2.5%, respectively. This confirms the efficiency of the proposed multi-level optimisation method.

3.4. Sensitivity to the selected acceleration record

In general, the sensitivity of the optimum design solution to the selected input acceleration record is one of the major obstacles for the practical applications of the existing seismic optimisation methods that use time history analyses. While optimal distribution of friction dampers under a specific acceleration record will not necessarily be optimal under another record, previous studies by Hajirasouliha and Moghaddam [53] and Hajirasouliha and Pilakoutas [54] on shear structures indicated that this can be sufficiently addressed by using a number of artificial earthquakes records consistent with the selected design spectrum. However, this means that rather than using one specific record, a number of acceleration records must be used simultaneously. An important issue is the number of acceleration records required to

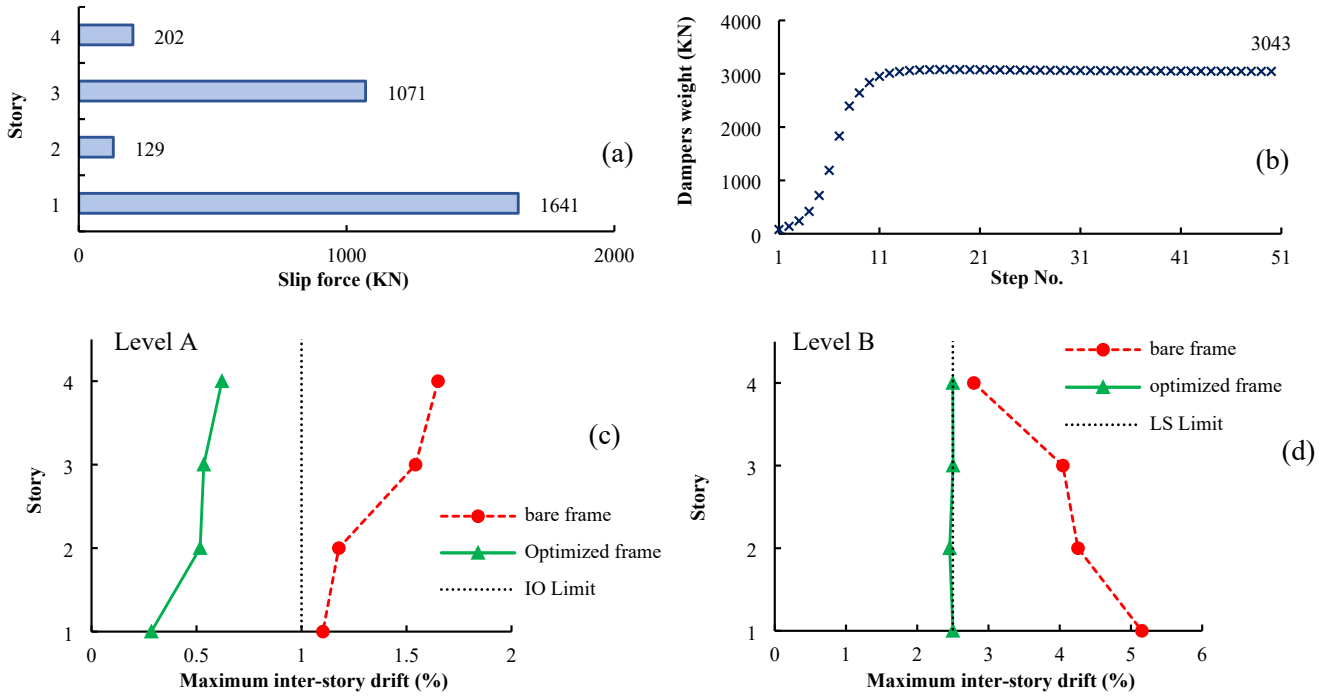

Fig. 7. Two-level optimisation for 4-story frame: (a) optimal distribution; (b) convergence trend of dampers weight; (c) maximum inter-story drifts in level A; (d) maximum inter-story drifts in level B.

achieve reliable results. For example, ATC58 [55] recommends that at least 11 records should be used. However, the greater the number of selected earthquake records, the greater the accuracy of the final solution. Therefore, in this study 22 natural earthquake records introduced by FEMA P-695 were utilized. The challenging issue is how to use these earthquake records in the adaptive optimisation process, which will be examined in the following.

3.4.1. *Using maximum slip threshold forces*

The first idea is to use maximum slip threshold forces required under

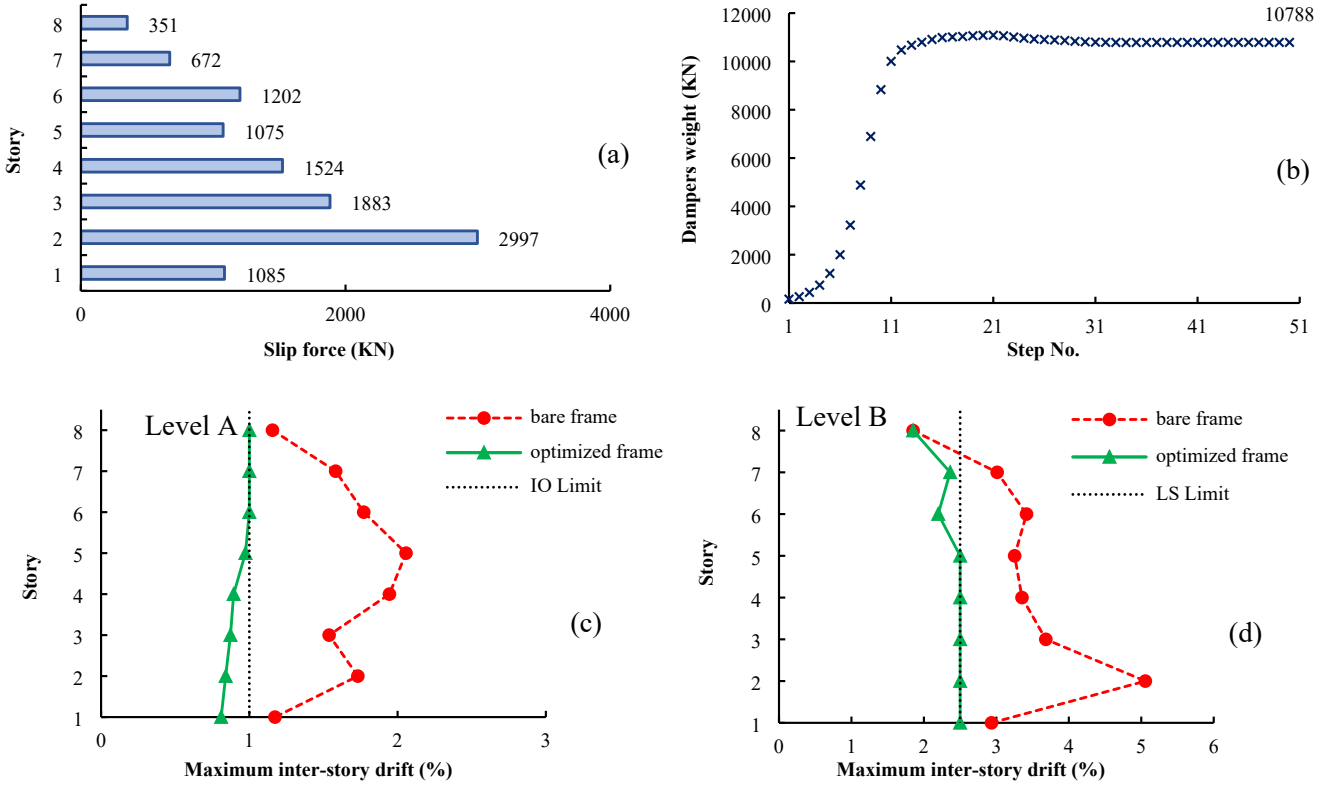

Fig. 8. Two-level optimisation for 8-story frame: (a) optimal distribution; (b) convergence trend of dampers weight; (c) maximum inter-story drifts in level A; (d) maximum inter-story drifts in level B.

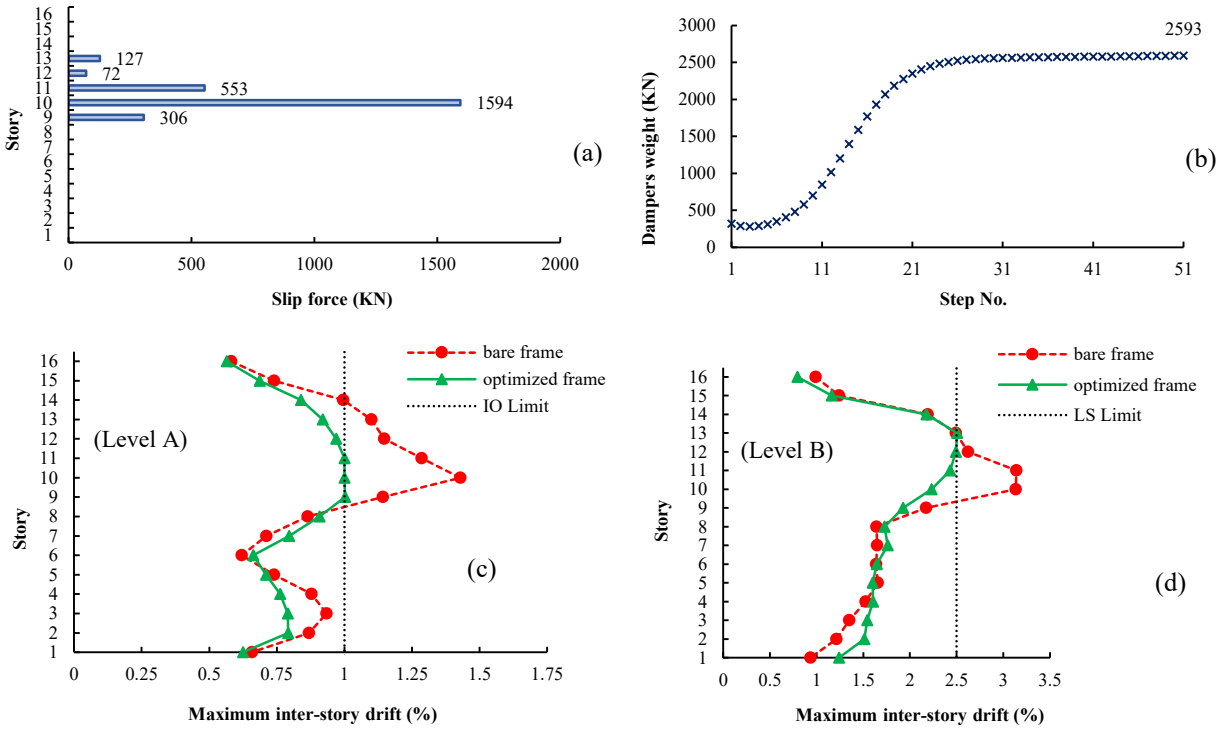

Fig. 9. Two-level optimisation for 16-story frame: (a) optimal distribution; (b) convergence trend of dampers weight; (c) maximum inter-story drifts in level A; (d) maximum inter-story drifts in level B.

the set of design earthquakes. This means that the optimisation process is firstly carried out for each acceleration records separately. Then the maximum slip threshold force of each story under all of the selected 22 records is used to design the damper of that story level. To evaluate the effectiveness of this idea, the proposed optimisation processes are conducted for 8-story frame under all the acceleration records, and the performance of the frame equipped with maximum dampers is determined. As it is seen in Fig. 10, the maximum inter-story drifts are considerably reduced in comparison to the bare frame, but the acceptance limit is exceeded at some story levels. One may expect that the problem can be easily solved by using stronger dampers. To assess the effectiveness of this approach, the frame is analyzed after using 1.1, 1.2, 1.3, 1.4, and 1.5 of times of the maximum slip threshold forces obtained in the previous step. As shown in Fig. 10, the optimisation criterion is not still satisfied. This highlights the need to look for a more appropriate design solution for such cases.

3.4.2. *Using reduced drift target range*

Another idea for simultaneous optimisation under several acceleration records is to reduce the range of acceptable maximum inter-story drift during the optimisation process. For this purpose, the acceptable maximum inter-story drift is reduced from 1.0% to 0.8% (i.e. 20% reduction). Then the 8-story frame is optimized for 22 records using the new inter-story drift target, and the maximum slip threshold force of the dampers at each story is considered. As shown in Fig. 11, the maximum inter-story drifts of the optimized frame in this case are lower than the permitted level, which means the optimisation criterion is satisfied. However, there appear to be two major problems: (1) The solution presented by this idea is accepted as a proper design, but it is not an optimal design; (2) The amount of drift reduction in different structures may vary, which means there is no specific criterion to estimate the required reduction in the drift target.

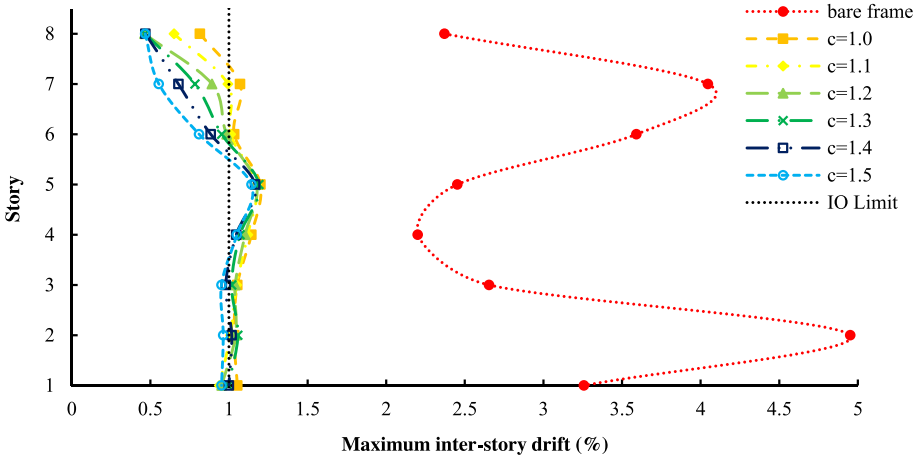

Fig. 10. Maximum inter-story drifts using maximum dampers.

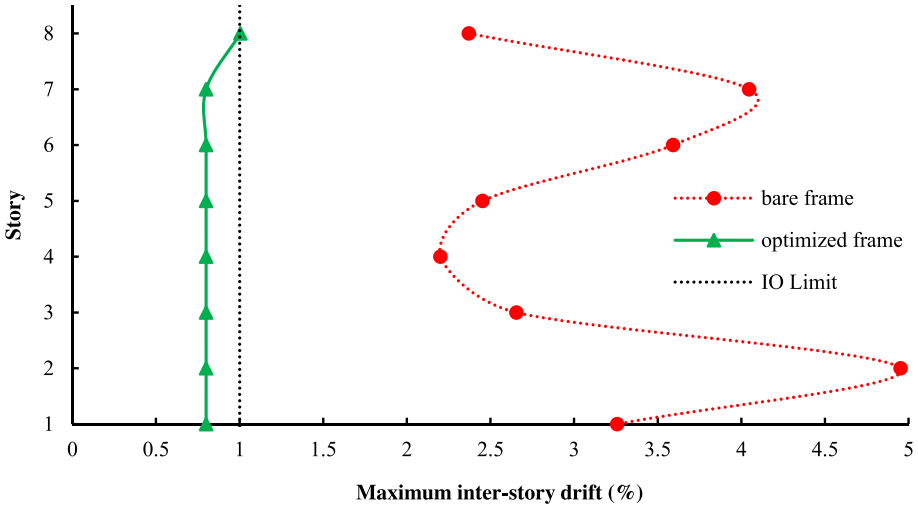

Fig. 11. Maximum inter-story drifts using reduced drift range.

3.4.3. *Improved adaptive optimisation technique*

To address the issues discussed above, this section aims to introduce an effective method for simultaneous optimisation of several acceleration records. For this purpose, Equation (5) is modified by using the following adaptation factor:

$$f\left(\frac{\delta}{\delta_t}\right)_i = \left(max\left(\left\{\left(\frac{Drift_{max}}{Drift_{target}}\right)_i |EQ1\right\}, \left\{\left(\frac{Drift_{max}}{Drift_{target}}\right)_i |EQ2\right\}, \cdots, \left\{\left(\frac{Drift_{max}}{Drift_{target}}\right)_i |EQn\right\}\right)\right)^{\beta} \tag{10}$$

where n is the number of acceleration records (here 22). Using this approach, the optimal distribution of friction dampers is obtained by satisfying the required seismic performance under all the selected records. If a large number of records are used (e.g. at least 11 records as recommended by ATC58 [55]), the results can be considered to be reliable.

The optimum distributions of the slip threshold forces are illustrated in Figs. 12(a), 13(a), and 14(a). It can be noticed that the optimum design solutions obtained for the 22 records are different compared to those calculated for one specific record. As shown in Figs. 12(b), 13(b), and 14(b), the dampers weights converged to the optimum values only after a few steps (7, 15 and 30 steps in the 4, 8, and 16-story frames, respectively). These results are also confirmed by the convergence process of COV shown in Fig. 12(d), 13(d), and 14(d), and highlight the computational efficiency of the proposed method. Comparison between the maximum inter-story drifts under all the 22 acceleration records before and after optimisation in Figs. 12(c), 13(c), and 14(c), indicates that the maximum inter-story drifts in the optimum design solutions reached the target value of 1% in all cases, and hence the optimisation criterion was satisfied. Fig. 12(e) to 14(e) and 12(f) to 14(f) show the dispersion of maximum inter-story drifts before and after the optimisation process. It can be seen that the maximum inter-story drifts significantly reduced in the optimum design solutions and are below 1.0% under all the selected input earthquake records.

3.5. *Probability curve*

Increasing the number of accelerations used in the optimisation process can potentially increase the reliability of the final design. To evaluate this, accelerations number 1 to 5 are considered for optimum design of the 8-story frame. The optimisation process is first performed for each record individually and the performance of the frame equipped with damper designed under one record is evaluated under the other 4 records. The same procedure is then repeated for simultaneous optimisation of 2, 3, 4, and 5 earthquake records. The results of the performance evaluation of the frame are presented in Fig. 15(a) using different number of earthquake input records. In this figure, the vertical axis is the probability of exceeding the permissible limit and the horizontal axis is the number of records used in the optimisation process. Note that for simultaneous optimisation of n accelerations, all possible modes for selecting n records from 5 records are considered. It is clear that as number of records increases, the probability of exceeding the limit reduces. It is seen that in the case optimizing is performed for all the 5 records simultaneously, 8-story frame does not exceed the drift limit under any of these 5 accelerations, and hence exceedance probability is zero. To provide more information, envelop of maximum inter-story drifts at each step are compared in Fig. 15(b) using different number of input records. It is obvious that increasing the number of acceleration records leads to a decrease in the maximum inter-story drifts experienced by the frame.

In order to generalize this conclusion, the optimal design solutions in this section were also evaluated under all the 22 selected acceleration records, and the results are presented in Fig. 15(c). It is shown that as the number of accelerations increases, the probability of exceeding the limit reduces. As expected, the exceedance probability has slightly increased compared to the cased only 5 records were used. However, it is evident that simultaneous optimisation using more than three records leads to relatively low exceedance probability levels acceptable for most practical applications. This is in consistent with the results reported by Domenico and Hajirasouliha [4] for steel frames equipped with nonlinear viscous dampers.

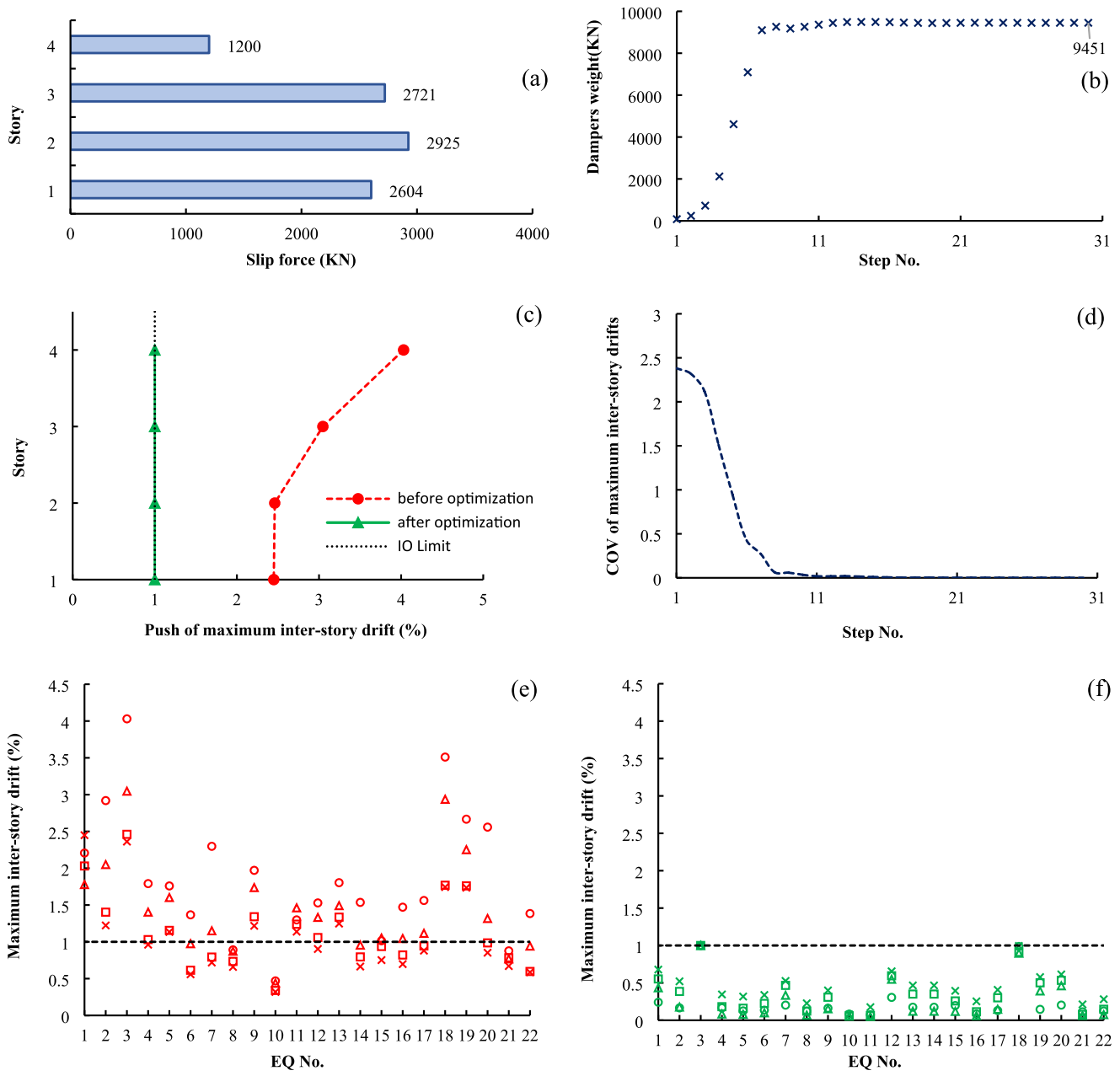

Fig. 12. Optimisation for multiple seismic excitations simultaneously for 4-story frame: (a) optimal distribution of slip threshold forces; (b) convergence trend of dampers weight; (c) maximum inter-story drifts; (d) convergence trend of COV; (e) dispersion of maximum inter-story drifts of bare frame under 22 accelerations; (f) dispersion of maximum inter-story drifts of optimum frame under 22 accelerations.

3.6. Control the adequacy of beams and columns

Increasing the stiffness of the structure, because of adding friction dampers, leads to increased applied forces to the structural members. Therefore, the adequacy of beams and columns after optimisation should be controlled. In this section, the adequacy of the members of the studied frames subjected to the set of 22 selected seismic excitations are evaluated. For this purpose, the demand to capacity ratio (DCR) of all members are determined based on ASCE/SEI41-13[41] regulations considering the Immediate Occupancy (IO) level as the objective structural performance level, using Equations (11) and (12).

$$\text{For beams}: DCR = \frac{\theta_p}{\theta_{all}} \tag{11}$$

$$\text{For Columns}: DCR = \begin{cases} \dfrac{\theta_p}{\theta_{all}} & \dfrac{P}{P_{cl}} \le 0.5 \\ \dfrac{P}{P_{cl}} + \dfrac{M}{M_{cl}} & \dfrac{P}{P_{cl}} > 0.5 \end{cases} \tag{12}$$

where θ_p and θ_{all} are the maximum plastic rotation and the allowable plastic rotation of the member, respectively. P and M are the maximum axial force and the maximum applied moment of the columns, while P_{cl} and M_{cl} are the allowable axial force and the allowable moment of the column based on AISC360-10 [56], respectively. The maximum value of DCR for each member under the set of 22 seismic excitations is shown in Fig. 16. DCR values below 0.01 are eliminated. It is clear that using the proposed optimisation method, the objective performance level is satisfied properly.

To provide more information, Fig. 17 compares the maximum plastic

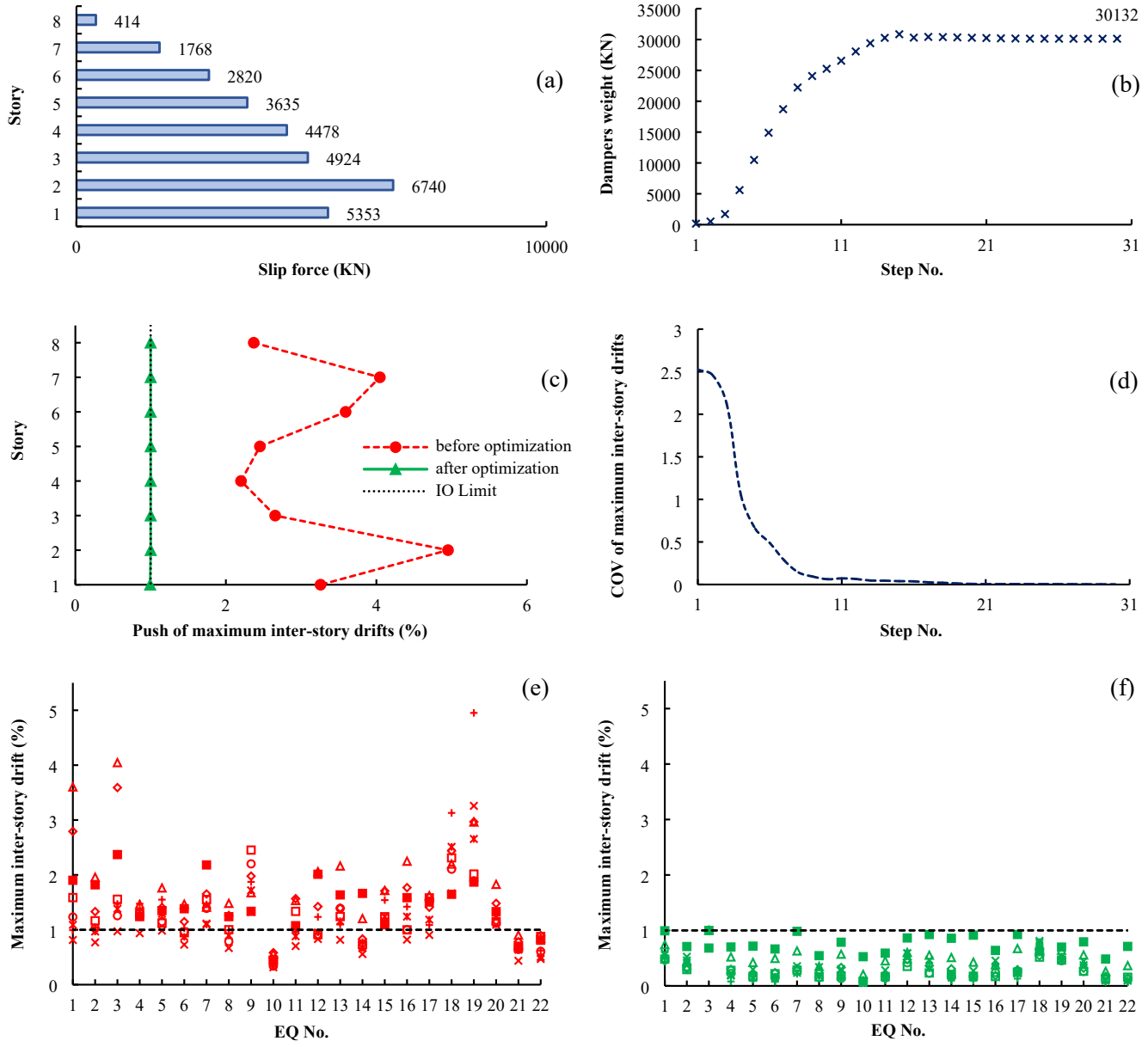

Fig. 13. Optimisation for multiple seismic excitations simultaneously for 8-story frame: (a) optimal distribution of slip threshold forces; (b) convergence trend of dampers weight; (c) maximum inter-story drifts; (d) convergence trend of COV; (e) dispersion of maximum inter-story drifts of bare frame under 22 accelerations; (f) dispersion of maximum inter-story drifts of optimum frame under 22 accelerations.

rotations of connected beams before and after adding dampers to the 4-story frame under the set of 22 selected seismic excitations. It can be seen that using the optimum design of friction dampers could significantly reduce the plastic rotations, and hence damage, in the structural elements by dissipating the seismic input energy through the friction mechanism.

It should be noted that the collapse mechanism of the frames was not directly controlled in this study. However, by adopting the proposed optimisation method, the displacement demands at different story levels are uniformly distributed and therefore any localized soft-story failure will be prevented. This is also expected to lead to higher collapse resistance of the frames by increasing the redundancy of the structure. Besides, the collapse resistance can be directly used as the key performance parameter in the optimum design process [57,58]. While this is not in the scope of this study, it can be a very good topic for further investigations.

3.7. Comparison with some other optimisation methods

This section evaluates the computational efficiency and accuracy of the adaptive optimisation method compared to standard optimisation methods, including an iterative method, a non-iterative method, and three metaheuristic methods. All these optimisation methods are applied for optimum design of friction dampers of the 4-story frame under one of the selected acceleration records (record number 17) and their results are compared with the adaptive optimisation technique.

3.7.1. Sung-Kyung Lee method

As explained in the introduction section, the Sung-Kyung Lee method [12] is based on minimizing the coefficient of Rd (see Equation (3)). The optimisation process is performed for different values of ρ1 and ρ2 under the selected acceleration record and the results are presented in Fig. 18. As can be seen, the minimum value for Rd (=0.41) is obtained when the distribution of the dampers is based on ρ1 = 0.45. To compare this

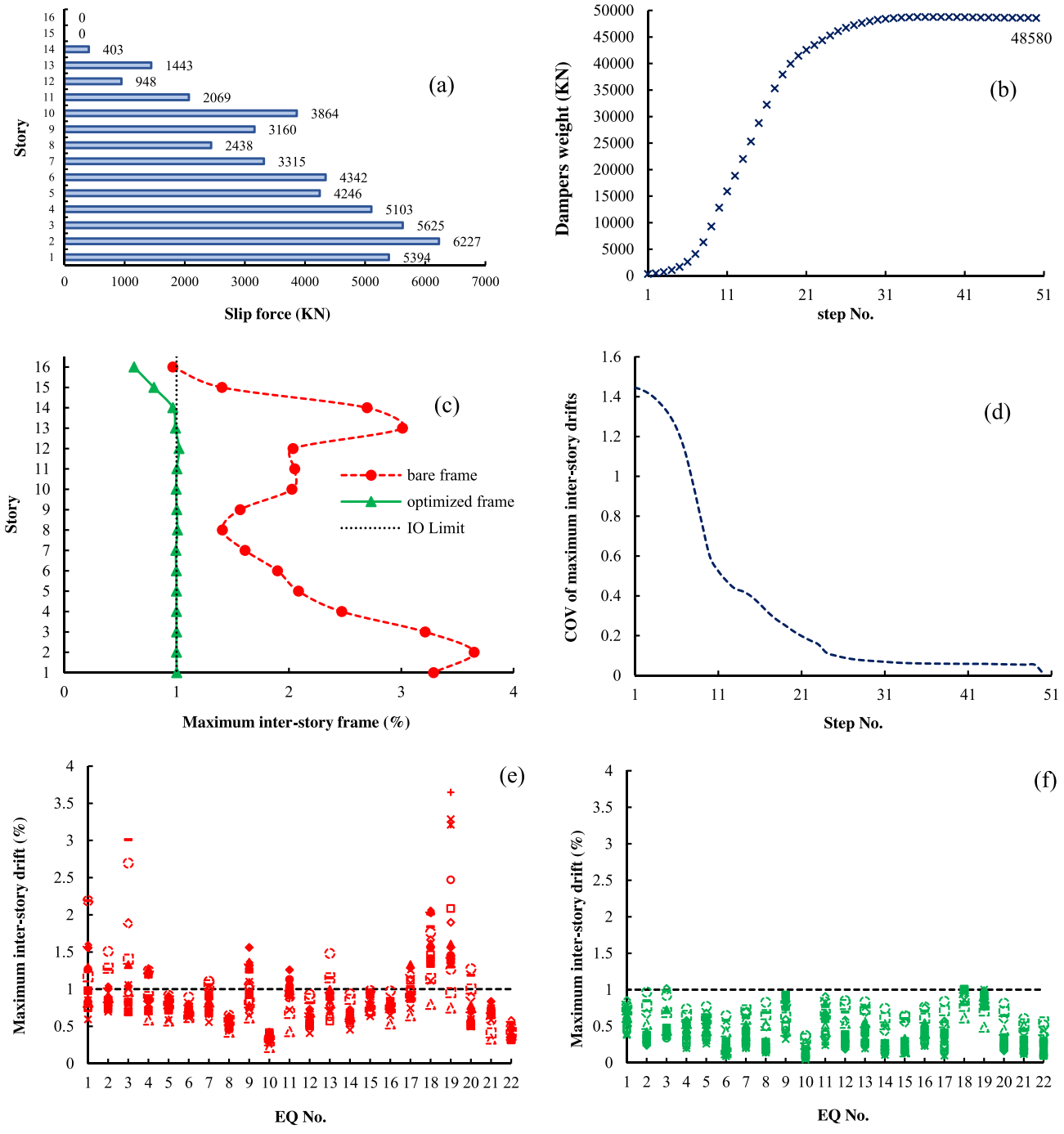

Fig. 14. Optimisation for multiple seismic excitations simultaneously for 16-story frame: (a) optimal distribution of slip threshold forces; (b) convergence trend of dampers weight; (c) maximum inter-story drifts; (d) convergence trend of COV; (e) dispersion of maximum inter-story drifts of bare frame under 22 accelerations; (f) dispersion of maximum inter-story drifts of optimum frame under 22 accelerations.

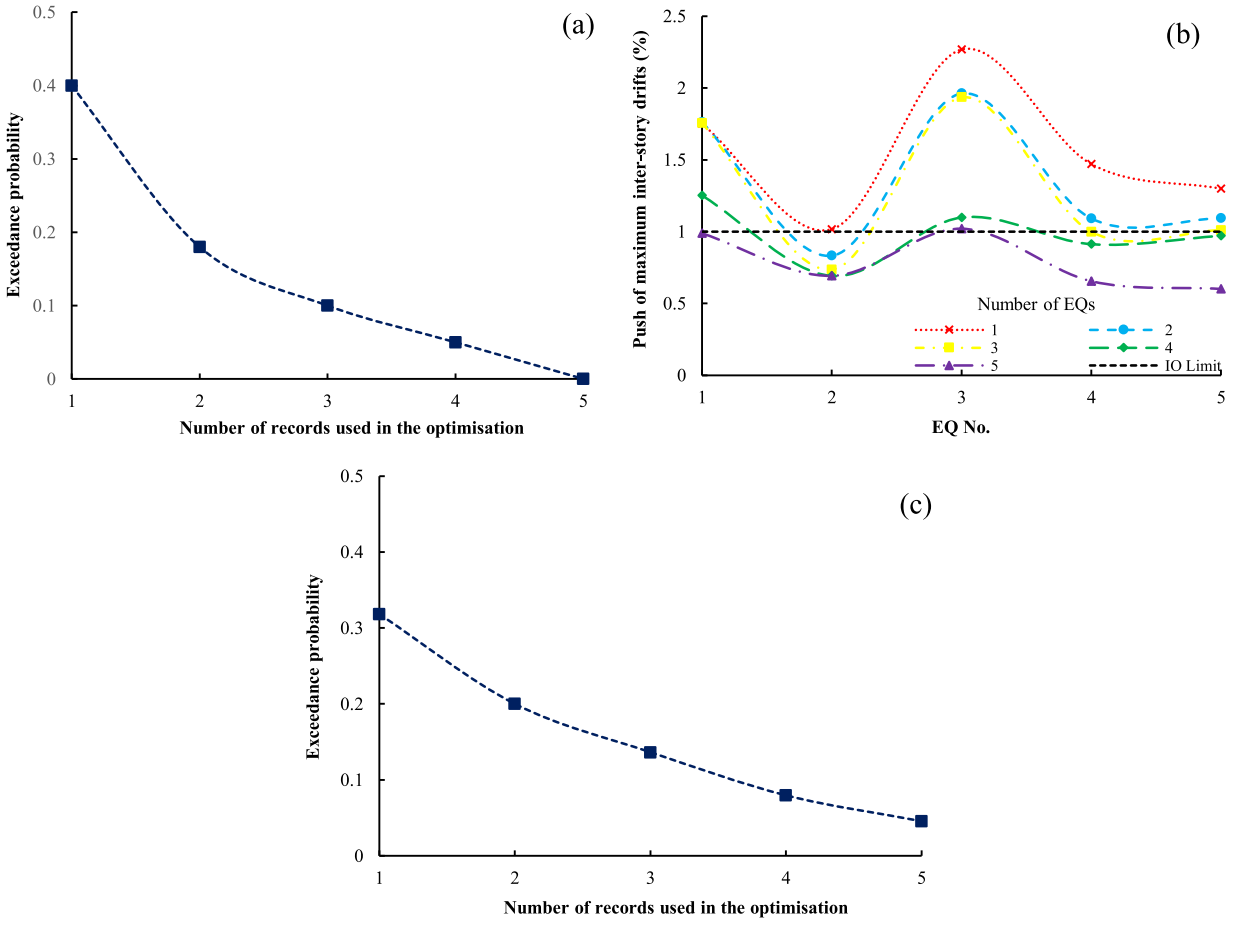

Fig. 15. Probability curves: (a) evaluation for 5 accelerations; (b) envelop of maximum inter-story drifts; (c) evaluation under 22 accelerations.

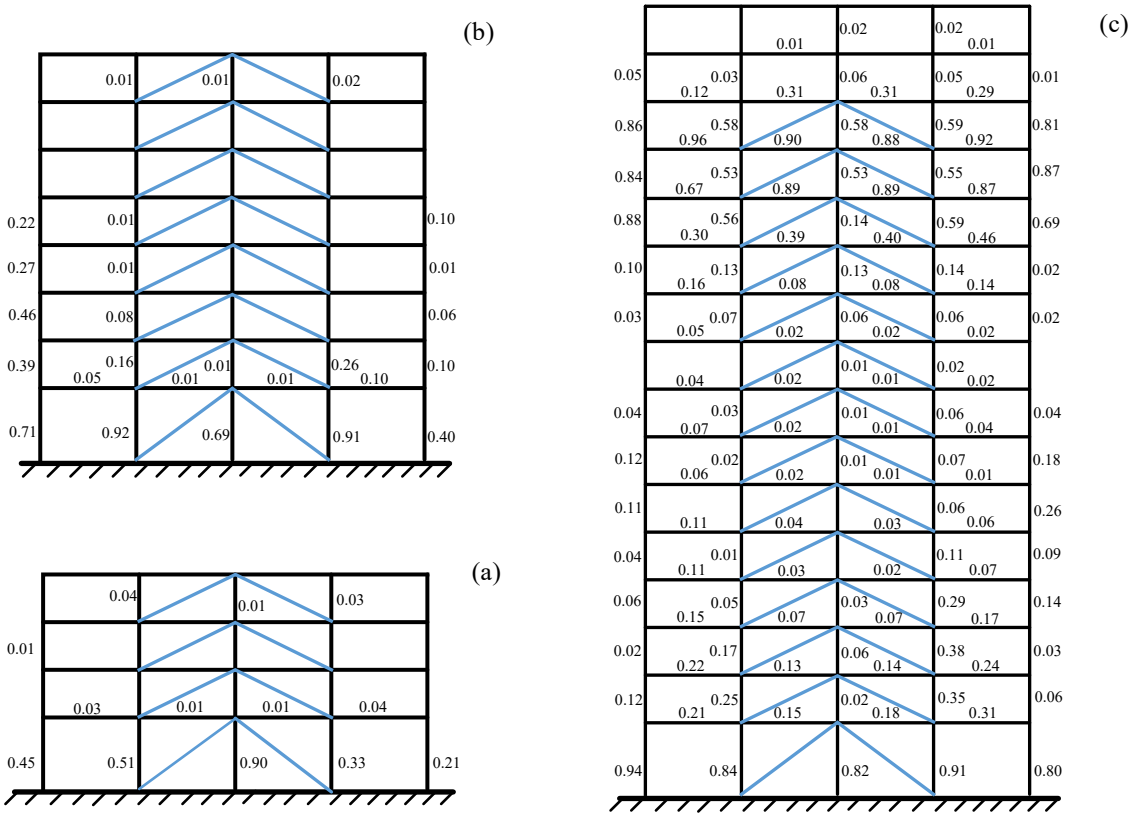

Fig. 16. Demand capacity ratio (DCR) of beams and columns of frames subjected to 22 seismic excitations.

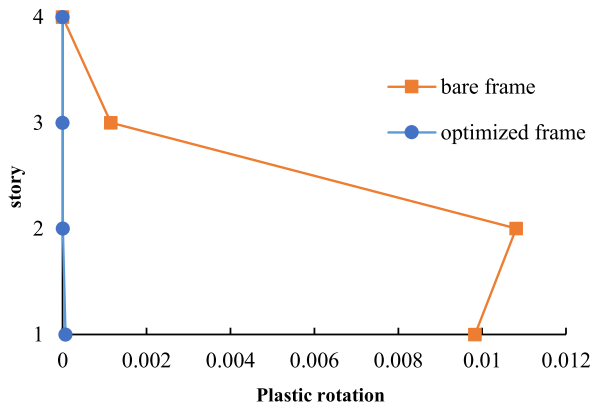

Fig. 17. Maximum plastic rotation of connected beams in the 4-story frame before and after using friction dampers subjected to 22 seismic excitations.

solution with the adaptive optimisation technique (AOT), the acceptance criterion Rd is set to 0.41 and the target maximum drift is determined using Equation (3). As can be seen in Fig. 18, by using the AOT the target Rd is achieved after around 30 steps, while in the Sung-Kyung Lee method less than 10 steps were required. This indicates that the Sung-Kyung Lee has a faster convergence rate, however, does not guarantee the efficiency of the final design. To assess this, the results of these two methods are compared in Fig. 19 in terms of maximum inter-story drift and slip force distribution. It can be seen that the required dampers weight in the Sung-Kyung Lee method is around 8834 kN, while it is reduced to 1838 kN in the AOT. This clearly indicates that the design obtained based on the adaptive optimisation technique is much more desirable since it requires significantly lower dampers weigh (80% less), and hence, exhibits lower bases shear and forces in the structural elements. It can be also noted that the AOT could efficiently identify the locations that the dampers are not required (here first story).

3.7.2. Baktash and Marsh method

One of the most frequently non-iterative optimisation methods used for friction dampers is Baktash and Marsh method [10], which is explained in the introduction section. Using equation (1), the optimum slip forces are calculated for different stories of the 4-story frame under the selected design acceleration. Fig. 20 shows the calculated slip forces and the inter-story drift distribution of the design solution in this case. For better comparison, the maximum inter-story drifts obtained by the Baktash and Marsh method [10] are considered as target drift values in the adaptive optimisation technique (AOT). The results of these two methods are compared in Fig. 20. It can be seen that the required dampers weight using the Baktash and Marsh method [10] and AOT were 7835 kN and 1077 kN, respectively. This indicates that the AOT could provide the same level of performance by only using about 14% of the dampers weight required in the design solution obtained by the Baktash and Marsh method [10]. This highlights again the efficiency of the AOT in obtaining the optimum slip forces in friction dampers.

3.7.3. Metaheuristic methods

In this section, three widely used metaheuristic optimisation methods, including genetic algorithm (GA), particle swarm optimisation algorithm (PSO), and simulated annealing algorithm (SA), are used to assess the adequacy of the AOT. These methods are generally expected to obtain the global optimum solutions by using different global searching strategies. To obtain the best design solution, the following objective function is minimized:

$$Objective\ Function = 100 \times \left(1 + \frac{1}{nStr}\sum_{i=1}^{nStr}\frac{S_i - S_{min}}{S_{max} - S_{min}}\right) \times \left(1 + \frac{1}{nStr}\sum_{i=1}^{nStr} g_i\right)^2 \tag{13}$$

$$g_i = \begin{cases} \dfrac{drift_i}{drift_{all}} - 1 & if\ drift_i \geq drift_{all} \\ 0 & otherwise \end{cases} \tag{14}$$

where nStr is the number of stories, S_i is design variable in i^{th} story, S_{min} and S_{max} are the minimum and maximum value of the design variable, respectively. g_i is the drift exceedance penalty parameter of i^{th} story, which is defined based on the drift of i^{th} story ($drift_i$) and the allowable drift value ($drift_{all}$). This parameter is used to ensure the final design solution satisfies the target performance target.

Using the abovementioned objective function, an optimisation code was developed in MATLAB software [59], to optimize the 4-story frame under the selected design acceleration (record number 17). In this study, each generation consisted of 50 number of randomly selected samples. To take into account the effects of the random selection of the initial samples, each of these methods was performed twice and the best solution was selected as the final design. Fig. 21 shows the variation of the objective functions as a function of number of analyses using different optimisation methods. The maximum inter-story drift distributions and the optimum slip threshold force of the friction dampers at different

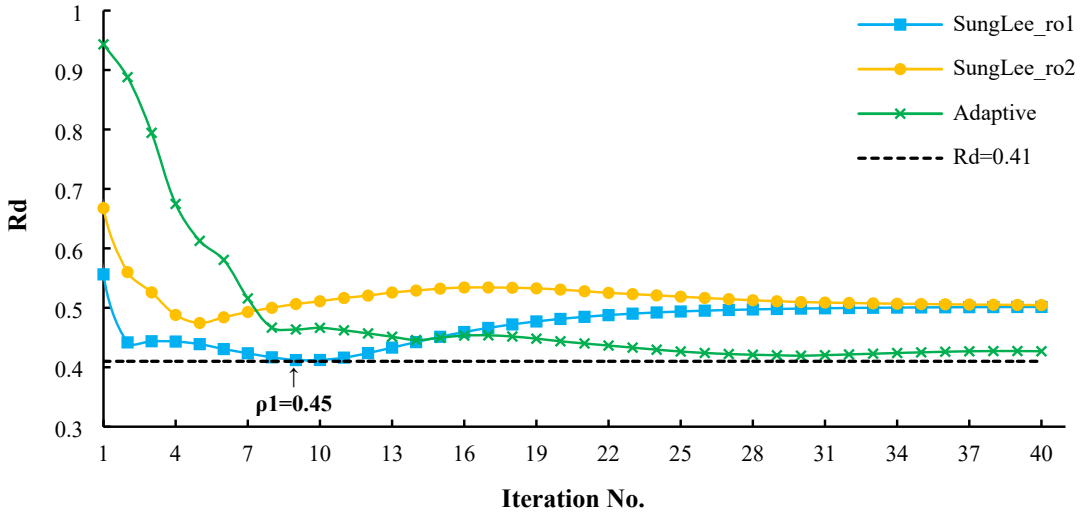

Fig. 18. Variation of Rd in optimisation process.

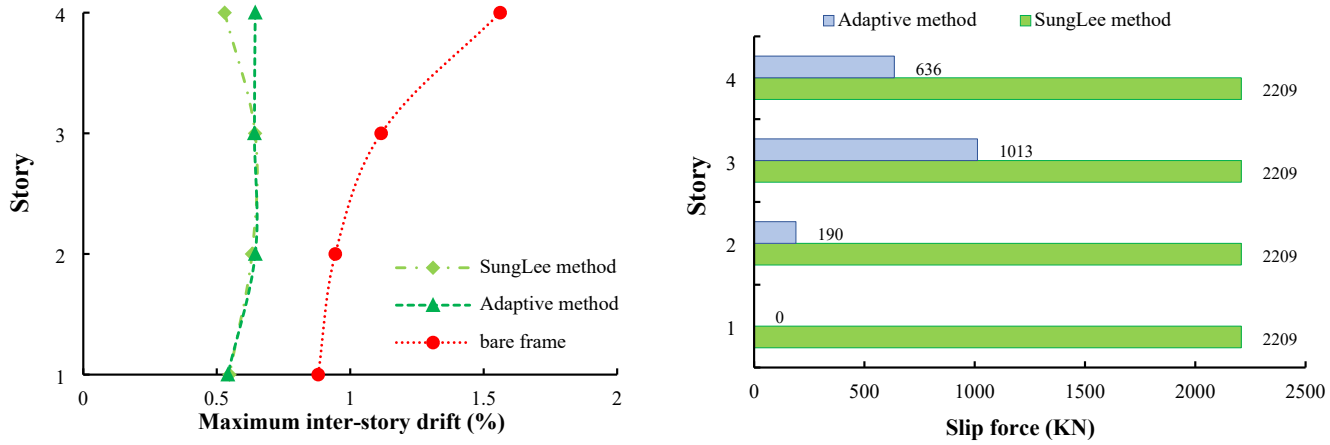

Fig. 19. Optimum design solutions obtained by the Adaptive and Sung-Kyung Lee [12] methods.

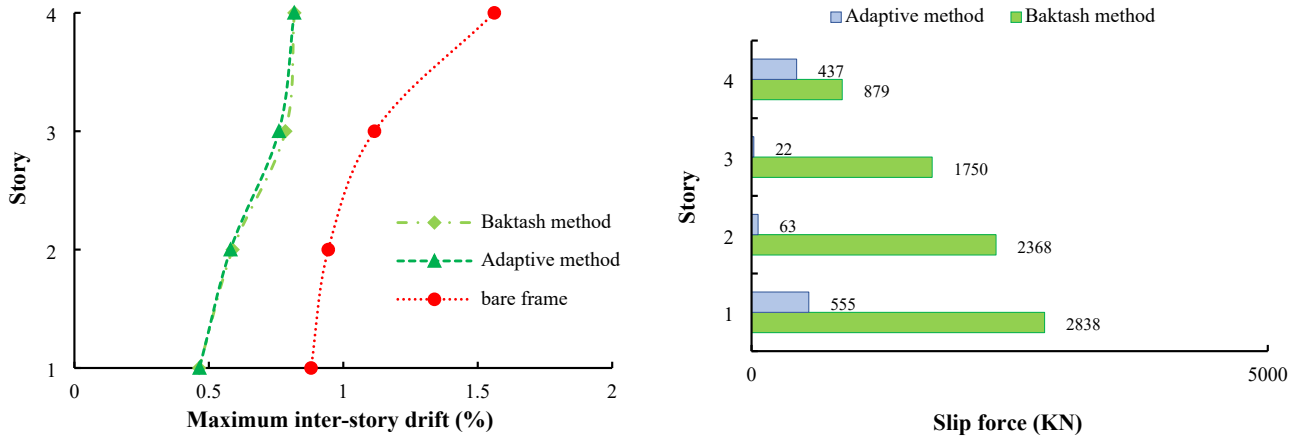

Fig. 20. Optimum design solutions obtained by the Adaptive and Baktash & Marsh [10] methods.

stories are also compared in Fig. 22. It can be seen that all the adopted optimisation methods reached an almost identical optimal solution, indicating the accuracy and efficiency of the proposed optimisation method. The inter-story drift distributions also indicate that the optimum design 4-story frame systems equipped with friction dampers satisfied the acceptance criterion. All the methods were also able to eliminate the inefficient dampers (by identifying the stories that do not need dampers to satisfy the target drift).

For better comparison, Table 6 compared the dampers weight, number of non-linear dynamic analyses, and the final objective function using different optimisation methods. It can be seen that the objective function and the dampers weight corresponding to each of these methods are approximately identical, but they differ in number of analyses required to obtain the optimal solution. In order to compare the number of analyses required in different algorithms, the objective function value of 1% higher than its optimal value was set as benchmark. According to the results, AOT, GA, PSO, and SA methods required 88, 1800, 2650 and 7510 non-linear dynamic analyses, respectively, to achieve the optimal solution. This clearly demonstrates the reliability and high computational efficiency of the proposed AOT compared to the metaheuristic optimisation methods, as it practically reached the same design solution by reducing the computational cost by at least 95%.

3.8. Non-symmetric frames

To optimize non-symmetric frames using adaptive optimisation technique (AOT), Equation (5) is modified to take into account the width of the bays. The convergence equation in this case defines as follows:

$$\left[(P_{SC})_i\right]_{n+1} = \left[(P_{SC})_i\right]_n \times \left(\frac{\overline{Drift_{max}}}{\overline{Drift_{target}}}\right)^{\beta} \times \left(\frac{\mu_i}{\overline{\mu}}\right)^{\alpha} \tag{15}$$

$$\overline{Drift_{max}} = \frac{1}{nd}\sum_{j=1}^{nd}(Drift_{max})_j \tag{16}$$

$$\overline{\mu} = \frac{1}{nd}\sum_{j=1}^{nd}(\mu)_j \tag{17}$$

where $\overline{Drift_{max}}$, $\overline{Drift_{target}}$ are the average of the maximum inter-story

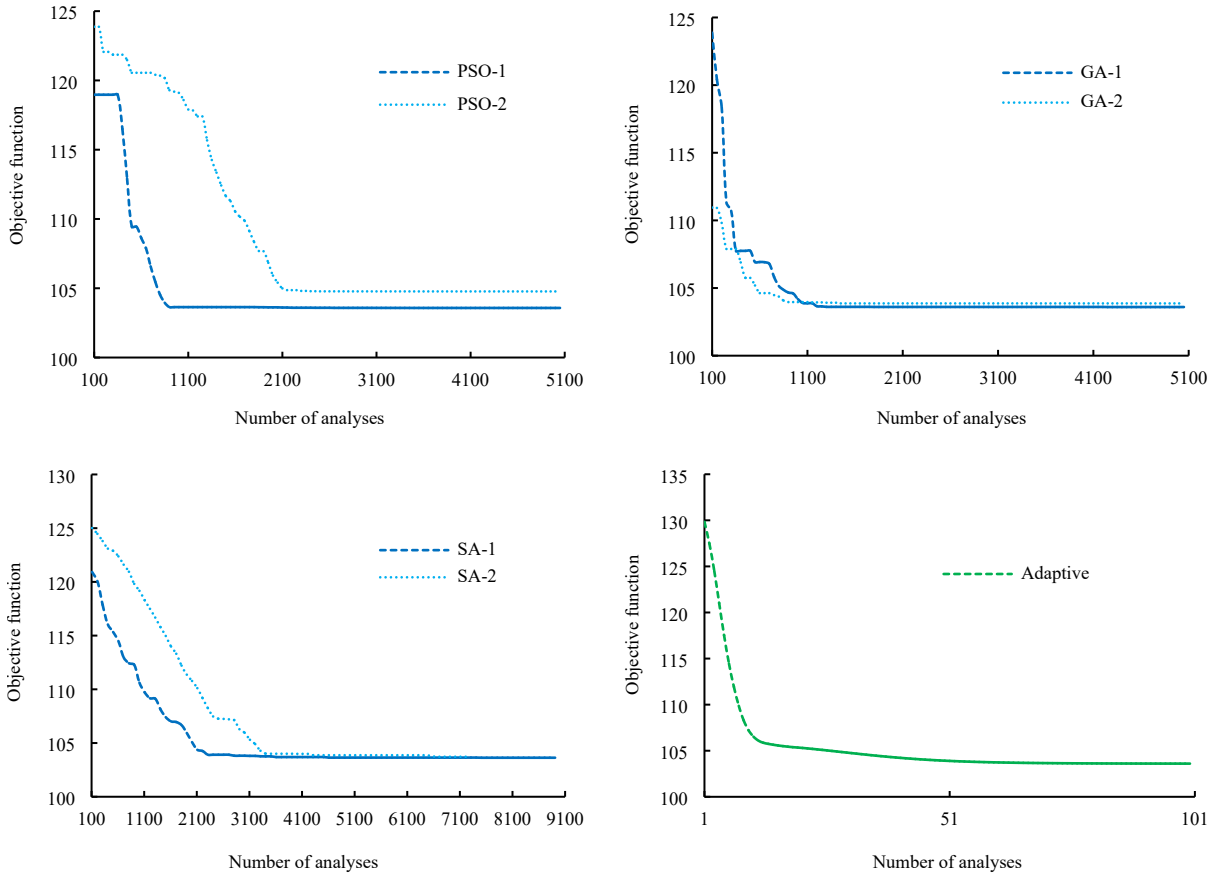

Fig. 21. Optimisation trend of metaheuristic algorithms and Adaptive optimisation technique.

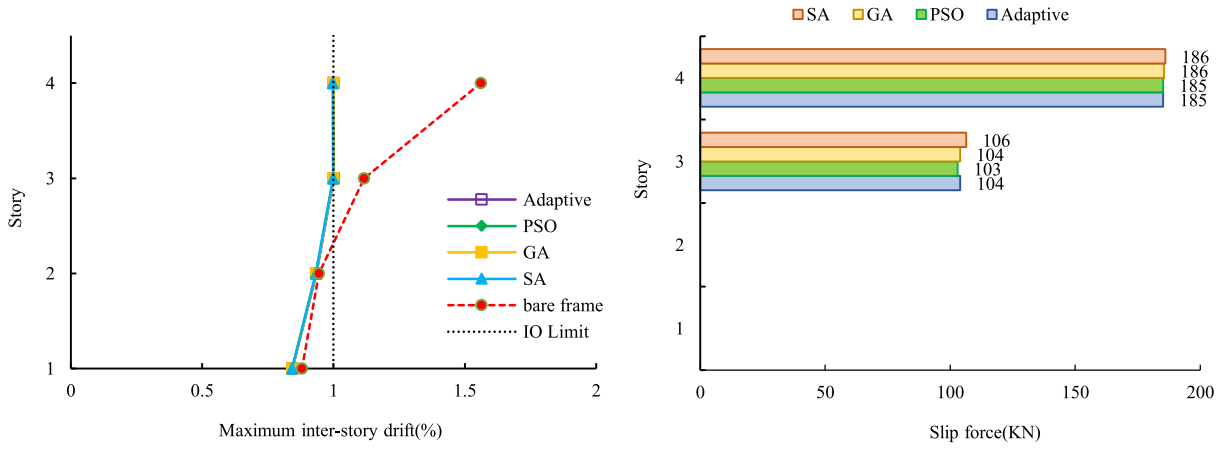

Fig. 22. Optimum design solutions obtained by the Metaheuristic and Adaptive optimisation techniques.

Table 6
Comparison of the optimum design solutions using PSO, GA, SA and Adaptive optimisation methods.

Optimisation Method	Dampers Weight (KN)	Number of Analyses	Objective Function
PSO	288	2650	103.5778
GA	290	1800	103.5955
SA	292	7510	103.6321
Adaptive	289	88	103.6002

drifts and average of the target inter-story drifts, respectively. *nd* represents the number of dampers, α and β are convergence coefficients, and μ is the inelastic deformation of each damper.

To demonstrate the efficiency of the method, 4, 8, 16 non-symmetric story frames shown in Fig. 23 are optimized under design earthquake No. 2. For non-symmetric optimisation, the dampers were moved to the side bays and the length of the side bays was changed to 4.57 m and 13.71 m.

The results of the optimisation of the non-symmetric 4, 8 and 16-story frames are shown in Fig. 24. Here the optimisation process is started by using a small slip threshold force (20 kN) in all dampers. It can be seen that using Equation (15) in the optimisation process leads to a quick convergence, especially in the shorter frames, while the inter-story drifts in the final design solutions are relatively uniform and less than the target value. The adopted method could also identify the unnecessary dampers. The results indicate that in non-symmetric frames, in general, the optimisation process reduces the slip threshold force of the dampers in the shorter bays and increases the slip threshold force of the dampers in the longer bays. As a result, all the dampers in the final solutions are placed in the longer bays. This can be justified since the diagonal elements in the longer bays provide larger horizontal force components, and therefore they are more efficient against lateral loads.

The outcomes of this study, in general, indicate that the proposed adaptive optimisation technique (AOT) can provide a low computational cost design tool for structural designers and practitioners to obtain the best position of the friction dampers and minimize their slip-threshold force to satisfy a predefined inter-story drift with minimum additional pressure on the existing structural elements. This is especially important when the friction diagonal dampers are utilized to retrofit existing SMRFs which suffer from poor seismic performance and sub-standard structural elements.

4. Summary and conclusions

A low computational cost framework called adaptive optimisation technique (AOT) was developed based on the theory of uniform distribution of damage (UDD) to achieve the optimal distribution of diagonal friction dampers installed in diagonal bracing elements in steel moment resisting frames (SMRFs) under seismic excitations. The efficiency of the proposed method was demonstrated through optimum design of 4, 8, and 16-story symmetric and non-symmetric SMRFs subjected to a set of strong natural earthquake records. Using the proposed optimisation method, the slip load and the effective location of dampers were optimized simultaneously, while the optimisation target was satisfied at all story levels. The results indicate that a range of 0.4 to 0.8 values for convergence coefficient, β, can guarantee the convergence in the case of optimisation of friction dampers. In most cases, only less than 20 steps were required to reach the optimum solution, while the final design was not affected by the optional starting point. Subsequently, the AOT was further developed to perform multi-level performance-based optimisation. It was shown that the proposed method could efficiently satisfy two different optimisation criteria, which were not necessarily in the same direction, under different earthquake intensity levels.

In general, the dependency of the optimum design solution to the selected design earthquake input is a challenge in practical applications. To address this issue, the efficiency of several methods was investigated using a set of 22 natural acceleration records. A novel approach was then proposed for simultaneous optimisation under multiple accelerations, and its efficiency was demonstrated for the optimum design of 4, 8, and 16-story frames.

To investigate the accuracy of the AOT, the results of the proposed method were compared with iterative, non-iterative, and three meta-heuristic optimisation methods, including Genetic Algorithm (GA), Particle Swarm Optimisation (PSO), and Simulated Annealing (SA).

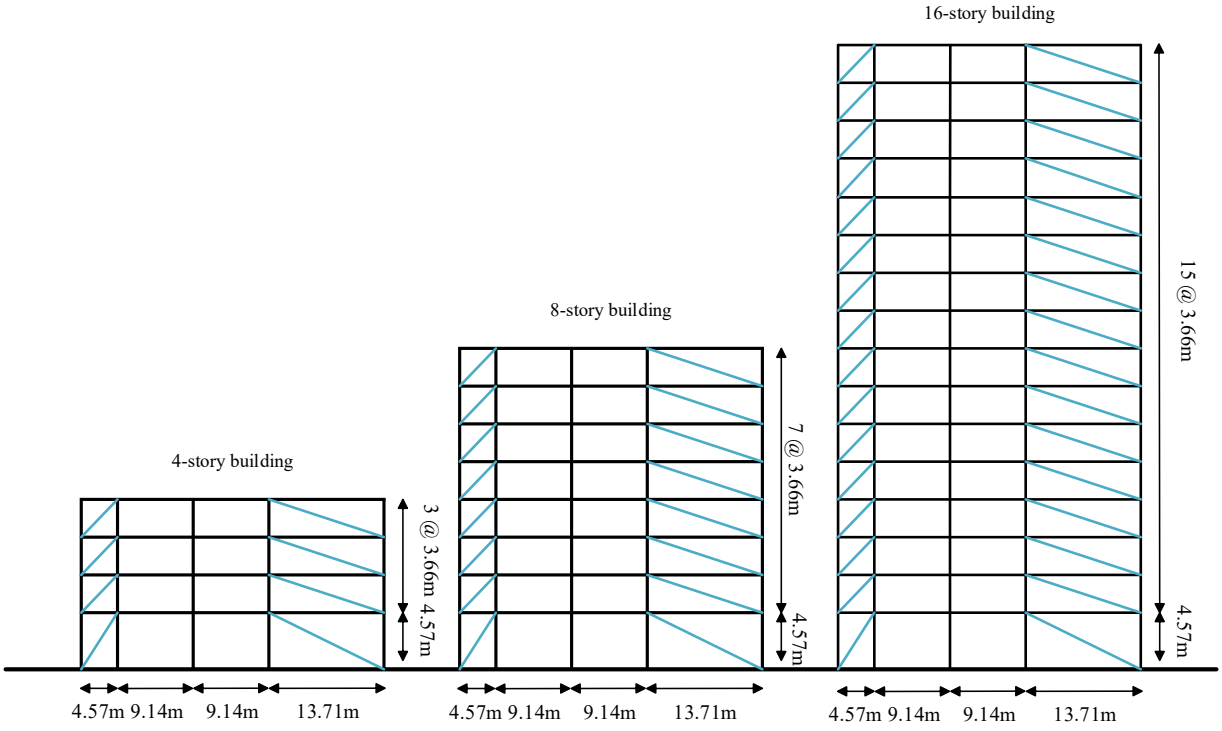

Fig. 23. Details of the non-symmetric 4, 8 and 16-story frames.

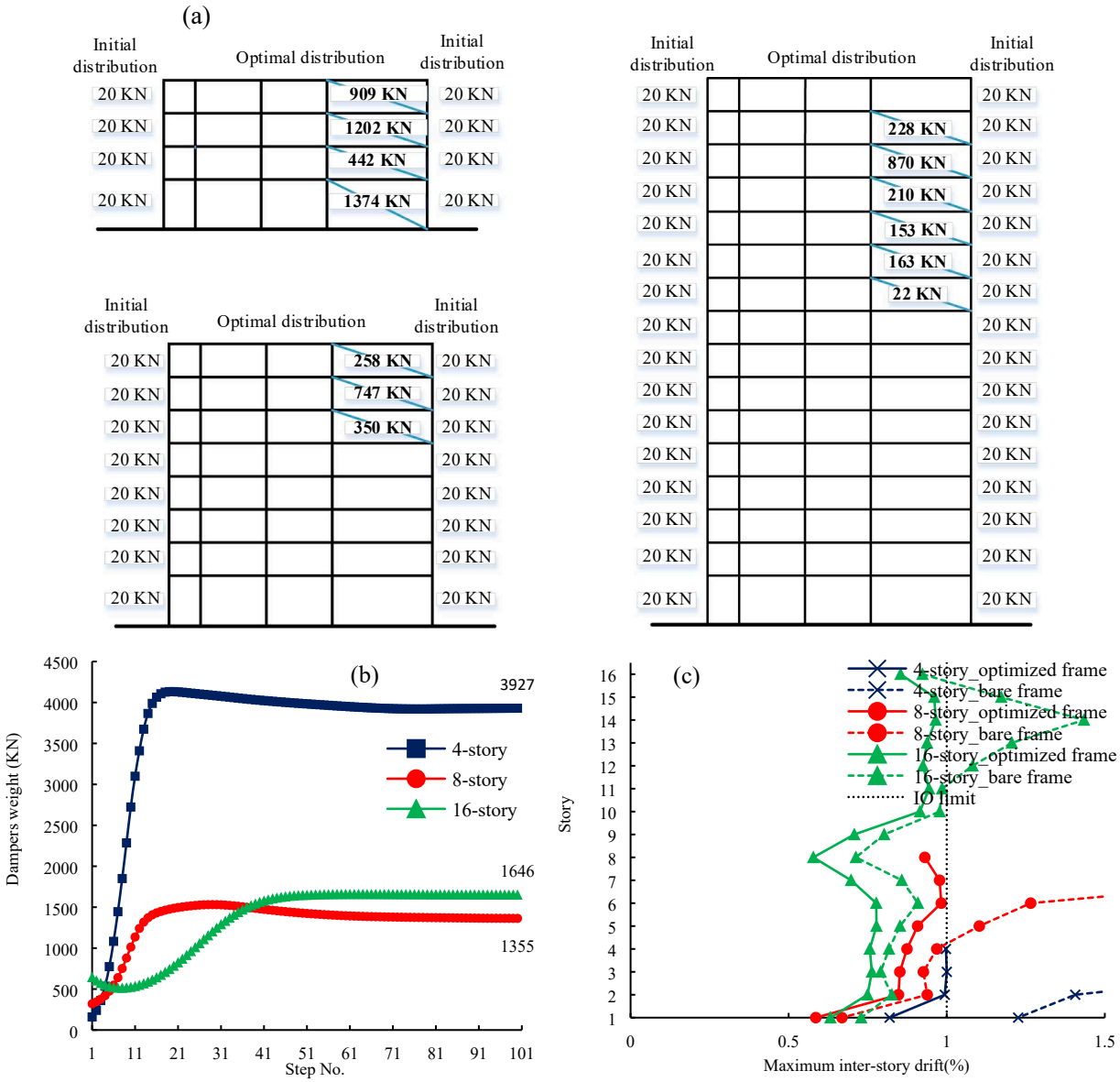

Fig. 24. Optimisation of the non-symmetric frames: (a) initial and optimal distribution of dampers; (b) convergence trend of dampers weight; (c) maximum inter-story drifts before and after optimisation.

According to the results, AOT, GA, PSO, and SA methods required 88, 1800, 2650 and 7510 non-linear dynamic analyses, respectively, to achieve the optimal solution. This clearly demonstrates the reliability and high computational efficiency of the proposed AOT compared to the metaheuristic optimisation methods, as it practically reached the same design solution by reducing the computational cost by at least 95%.

The AOT was also adopted to optimize non-symmetric (in bays) SMRFs. The results indicated that in non-symmetric frames, in general, the optimisation process reduced (or eliminated) the slip threshold force of the dampers in the shorter bays and increases the slip threshold force of the dampers in the longer bays.

Declaration of Competing Interest

The authors declare that they have no known competing financial interests or personal relationships that could have appeared to influence the work reported in this paper.

References

[1] Nishimura I. Performance evaluation of damping devices installed in a building structure. J Struct Constr Eng – Trans Arch Inst Jpn 2004;579:23–30.
[2] Symans MD, Charney FA, Whittaker AS, Constantinou MC, Kircher CA, Johnson MW, et al. Energy dissipation systems for seismic applications: current practice and recent developments. J Struct Eng – ASCE 2008;134(1):3–21.
[3] Lavan O, Dargush GF. Multi-objective evolutionary seismic design with passive energy dissipation systems. J Earthquake Eng 2009;13(6):758–90.
[4] De Domenico D, Hajirasouliha I. Multi-level performance-based design optimisation of steel frames with nonlinear viscous dampers. Bull Earthq Eng 2021; 19(12):5015–49.
[5] Nishimura I. Performance evaluation of a building structure with nonlinear dampers under strong ground motion on March 11, 2011. 14th US-Japan workshop on improvement of structural design and construction practices, Wailea-Makena Hawaii. 2012.
[6] Pall A. Limited slip bolted joints, a device to control the seismic response of large panel structures. PhD Thesis. Montreal, QC: Building, Civil and Environmental Engineering, Concordia University; 1979.
[7] Roik K, Dorka U, Dechent P. Vibration control of structures under earthquake loading by three-stage friction-grip elements. Earthquake Eng Struct Dyn 1988;16 (4):501–21.
[8] Lukkunaprasit P, Wanitkorkul A, Filiatrault A. "Performance deterioration of slotted-bolted connection due to bolt impact and remedy by restraints", In 13th

World Conference on Earthquake Engineering, Vancouver, Canada, B.C. No. 1986 (2004).
[9] Morales Ramirez JD, Tirca L, "Numerical simulation and design of friction-damped steel frame structures", In 15th World Conference on Earthquake Engineering, Lisbon, Portugal (2012).
[10] Baktash P, Marsh C. "Seismic behavior of friction damped braced frames". In Proc. 3rd U.S. National Conference on Earthquake Engineering. Charleston, SC, 1099-1105 (1986).
[11] Moreschi LM. Seismic Design of Energy Dissipation Systems for Optimal Structural Performance. Blacksburg, Virginia: Virginia Polytechnic Institute; 2000. Ph.D. Thesis.
[12] Lee S-K, Park J-H, Moon B-W, Min K-W, Lee S-H, Kim J. Design of a bracing-friction damper system for seismic retrofitting. Smart Struct Syst 2008;4(5):685–96.
[13] Nabid N, Hajirasouliha I, Petkovski M. Adaptive low computational cost optimization method for performance-based seismic design of friction dampers. Eng Struct 2019;198:109549.
[14] Nabid N, Hajirasouliha I, Petkovski M. A practical method for optimum seismic design of friction wall dampers. Earthq Spectra 2017;33(3):1033–52.
[15] Nabid N, Hajirasouliha I, Escolano Margarit D, Petkovski M. Optimum energy based seismic design of friction dampers in RC structures. Structures 2020;27:2550–62.
[16] Nabid N, Hajirasouliha I, Petkovski M. Performance-based optimisation of RC frames with friction wall dampers using a low-cost optimisation method. B Earthq Eng 2018;16(10):5017–40.
[17] Nabid N, Hajirasouliha I, Petkovski M. Simplified method for optimal design of friction damper slip loads by considering near-field and far-field ground motions. J Earthq Eng 2021;25(9):1851–75.
[18] Nastri E, D'Aniello M, Zimbru M, Streppone S, Landolfo R, Montuori R, et al. Seismic response of Steel Moment Resisting Frames equipped with friction beam-to-column joints. Soil Dyn Earthquake Eng 2019;119:144–57. https://doi.org/10.1016/j.soildyn.2019.01.009.
[19] Di Lauro F, Montuori R, Nastri E, Piluso V. Partial safety factors and overstrength coefficient evaluation for the design of connections equipped with friction dampers. Eng Struct 2019;178:645–55.
[20] Tartaglia R, D'Aniello M, Campiche A, Latour M. Symmetric friction dampers in beam-to-column joints for low-damage steel MRFs. J Constr Steel Res 2021;184:106791.
[21] Longo A, Montuori R, Piluso V. Theory of plastic mechanism control for MRF-CBF dual systems and its validation. Bull Earthq Eng 2014;12(6):2745–75. https://doi.org/10.1007/s10518-014-9612-2.
[22] Montuori R, Nastri E, Piluso V. Advances in theory of plastic mechanism control: closed form solution for MR-Frames. Earthquake Eng Struct Dyn 2015;44(7):1035–54. https://doi.org/10.1002/eqe.2498.
[23] Piluso V, Montuori R, Nastri E, Paciello A. Seismic response of MRF-CBF dual systems equipped with low damage friction connections. J Constr Steel Res 2019;154:263–77. https://doi.org/10.1016/j.jcsr.2018.12.008.
[24] Moghaddam H. Earthquake engineering (1st Edition). Tehran, Iran: RTRC; 1996.
[25] Moghaddam H. On the Optimum Performance-Based Design of Structures. In: Proceedings of U.S.-Iran Seismic Workshop on "Improving Earthquake Mitigation through Innovations and Applications in Seismic Science, Engineering, Communication, and Response", June 29–July 1, Irvine, California; 2009. p. 175–203.
[26] Moghaddam H, Hajirasouliha I. Fundamentals of Optimum performance-based design for dynamic excitations. J Sci Iran 2005;12(4):368–78.
[27] Moghaddam H, Hajirasouliha I. Toward more rational criteria for determination of design earthquake forces. Int J Solids Struct 2006;43(9):2631–45.
[28] Hajirasouliha I, Asadi P, Pilakoutas K. An efficient performance-based seismic design method for reinforced concrete frames. Earthquake Eng Struct Dyn 2012;41(4):663–79.
[29] Mohammadi RK, Mirjalaly M, Mirtaheri M, Nazeryan M. Comparison between uniform deformation method and genetic algorithm for optimising mechanical properties of dampers. Earthq Struct 2018;14(1):1–10.
[30] Lavan O. A methodology for the integrated seismic design of nonlinear buildings with supplemental damping. Struct Control Health Monit 2015;22(3):484–99.
[31] Moghaddam H, Hajirasouliha I, Hosseini Gelekolai SM. Performance-based seismic design of moment resisting steel frames: adaptive optimisation framework and optimum design load pattern. J Struct 2021;33:1690–704.
[32] Karami Mohammadi R, El Naggar MH, Moghaddam H. Optimum strength distribution for seismic resistant shear-buildings. Int J Solids Struct 2004;41(22-23):6597–612.
[33] Moghaddam H, Hajirasouliha I, Doostan A. Optimum seismic design of concentrically braced steel frames: concepts and design procedures. J Constr Steel Res 2005;61(2):151–66.
[34] Hajirasouliha I, Pilakoutas K, Moghaddam H. Topology optimisation for the seismic design of truss-like structures. Comput Struct 2011;89(7–8):702–11.
[35] Moghaddam H, Hajirasouliha I. Optimum strength distribution for seismic design of tall buildings. Struct Des Tall Special Build 2008;17(2):331–49.
[36] Hajirasouliha I, Pilakoutas K, Mohammadi RK. Effects of uncertainties on seismic behaviour of optimum designed braced steel frames. Steel Compos Struct 2016;20(2):317–35.
[37] Moghaddam H, Mohammadi RK. More efficient seismic loading for multidegrees of freedom structures. J Struct Eng 2006;132(10):1673–7.
[38] Moghadam H, Hajirasouliha I. Fundamentals of optimum performance-based design for dynamic excitations. Scientia Iranica 2005;12(4):368–78.
[39] Mohammadi RK, Sharghi AH. On the optimum performance-based design of eccentrically braced frames. Steel Compos Struct 2014;16(4):357–74.
[40] Moghaddam H, Hosseini Gelekolai SM, Hajirasouliha I. More efficient lateral load patterns for seismic design of steel moment-resisting frames. Struct Build 2018;171(6):487–502.
[41] ASCE (American Society of Civil Engineers) (2013) ASCE/SEI41-13: Seismic rehabilitation of existing buildings. American Society of Civil Engineers, Virginia, USA.
[42] Jin J, El-Tawil S. Seismic performance of steel frames with reduced beam section connections. J. Constr Steel Res 2004;61:453–71.
[43] Ghassemieh M, Kiani J. Seismic evaluation of reduced beam section frames considering connection flexibility. Struct Des Tall Spec Build 2012;22:1248–69.
[44] Kildashti K, Mirghaderi R, Kani IM. The efficiency of reduced beam section connections for reducing residual drifts in moment resisting frames. Open J Civ Eng 2012;02(02):68–76.
[45] Naughton DT, Tsavdaridis KD, Maraveas Ch, Nicolaou A. Pushover Analysis of Steel Seismic Resistant Frames with Reduced Web Section and Reduced Beam Section Connections. J Frontiers Built Environment October 2017:06. https://doi.org/10.3389/fbuil.2017.00059.
[46] FEMA 302. (1997). "Part 1 Provisions – NEHRP "Recommended Provisions for Seismic Regulations for New Buildings and Other Structures," in Building Seismic Safety Council-BSSC, Washington, DC: The Federal Emergency Management Agency.
[47] FEMA 350. (2000a). "Recommended seismic design criteria for new steel moment-frame buildings," in Connection Qualification, Prepared for the SAC Joint Venture, Chap. 3, Washington, DC: The Federal Emergency Management Agency, American Society of Civil Engineers-ASCE.
[48] American Institute of Steel Construction, Inc. (2016). Seismic Provisions for Structural Steel Buildings, ANSI/AISC Standard 341-16. Chicago, IL: AISC.
[49] OpenSees (Open System for Earthquake Engineering Simulation) (2015) University of California, Berkeley: PEER (Pacific Earthquake Engineering Research Center) http://opensees.berkeley.edu.
[50] FEMA P695. (2009). Quantification of building seismic performance factors. Report No. P695, Federal Emergency Management Agency, Washington, D.C.
[51] PEER (Pacific Earthquake Engineering Research Center) (2010) PEER Ground Motion Database. University of California, Berkeley, USA. http://peer.berkeley.edu/smcat/search.html.
[52] FEMA P-2082-1, "NEHRP Recommended Seismic Provisions for New Buildings and Other Structures 2020 Edition: Vol 1: Part 1 Provisions, Part 2 Commentary, 2020.
[53] Hajirasouliha I, Moghaddam H. New lateral force distribution for seismic design of structures. J Struct Eng ASCE 2009;135(8):906–15.
[54] Hajirasouliha I, Pilakoutas K. General seismic load distribution for optimum performance-based design of shear-buildings. J Earthquake Eng 2012;16(4):443–62.
[55] Applied Technology Council (ATC), Seismic performance assessment of buildings (ATC-58), Applied Technology Council (ATC), Redwood City, CA, USA, 2009.
[56] American Institute of Steel Construction (AISC) (2010) Specification for Structural Steel Buildings. An American National Standard. ANSI/AISC 360-10.
[57] Li S, Yu B, Gao M, Zhai C. Optimum seismic design of multi-story buildings for increasing collapse resistant capacity. Soil Dyn Earthquake Eng 2019;116:495–510.
[58] Gao M, Li S. Refined Seismic Design Method for RC frame structures to increase the collapse resistant capacity. Appl Sci 2020;10(22):8230. https://doi.org/10.3390/app10228230.
[59] MATLAB, version R2016b. The Math Works Inc 2016 Natick, Massachusetts, USA.